Final Report of

Collaborative Research:
Fundamental Science of Low Temperature Plasma-Biological Material Interactions

(Award# DESC0005105 and DE-SC0004664)

September 2014

Principal and co-principal investigators

University of Maryland, College Park, Profs. G. S. Oehrlein and J. Seog

UC Berkeley, Profs. D. Graves and J.-W. Chu

Table of Contents

Executive Summary

Low temperature plasma (LTP) treatment of biological tissue is a promising path toward sterilization of bacteria due to its versatility and ability to operate under well-controlled and relatively mild conditions. The present collaborative research of an interdisciplinary team of investigators at University of Maryland, College Park (UMD), and University of California, Berkeley (UCB) focused on establishing our knowledge based with regard to low temperature plasma-induced chemical modifications in biomolecules that result in inactivation due to various plasma species, including ions, reactive radicals, and UV/VUV photons. The overall goals of the project were to identify and quantify the mechanisms by which low and atmospheric pressure plasma deactivates endotoxic biomolecules. Additionally, we wanted to understand the mechanism by which atmospheric pressure plasmas (APP) modify surfaces and how these modifications depend on the interaction of APP with the environment. Various low pressure plasma sources, a vacuum beam system and several atmospheric pressure plasma sources were used to accomplish this.

In our work we elucidated for the first time the role of ions, VUV photons and radicals in biological deactivation of representative biomolecules, both in a UHV beam system and an inductively coupled, low pressure plasma system, and established the associated atomistic biomolecule changes. While we showed that both ions and VUV photons can be very efficient in deactivation of biomolecules, significant etching and/or deep modification (~200 nm) accompanied these biological effects. One of the most important findings in this work is the significant radical-induced deactivation and surface modification can occur with minimal etching. However, if radical fluxes and corresponding etch rates are relatively high, for example at atmospheric pressure, endotoxic biomolecule film inactivation may require near-complete removal of the film.

These findings motivated further work at atmospheric pressure using several types of low temperature plasma sources, for which radical induced interactions generally dominate due to short mean free paths of ions and VUV photons. For these conditions we demonstrated the importance of environmental interactions when atmospheric pressure plasma sources are used to modify biomolecules. This is evident from both gas phase characterization data and *in-situ* surface characterization of treated biomolecules. Environmental interactions can produce unexpected outcomes due to the complexity of reactions of reactive species with the atmosphere which determines the composition of reactive fluxes and atomistic changes of biomolecules.

Overall, this work clarified a richer spectrum of scientific opportunities and challenges for the field of low temperature plasma-biomolecule surface interactions than initially anticipated, in particular for plasma sources operating at atmospheric pressure. The insights produced in this work, e.g. demonstration of the importance of environmental interactions, are generally important for applications of APP to materials modifications. Thus one major contributions of this research has been the establishment of methodologies to more systematically study the interaction of plasma with bio-molecules. In particular, our studies of atmospheric pressure

plasma sources using very well-defined experimental conditions enabled to combine atomistic surface modifications of biomolecules with changes in their biological function. The clarification of the role of ions, VUV photons and radicals in deactivation of biomolecules during low pressure and atmospheric pressure plasma-biomolecule interaction has broad implications, e.g. for the emerging field of plasma medicine. The development of methods to detect the effects of plasma treatment on immune-active biomolecules will be helpful in many future studies.

Year 1 Progress Report, May 2011: Activities and Findings

Overview

Low temperature plasma (LTP) treatment of biological tissue is a promising path toward sterilization of bacteria due to its versatility and ability to operate under well-controlled and relatively mild conditions [1]. Past works have shown plasma-induced degradation of bacteria [2], but little knowledge exists regarding the plasma-induced chemical modifications in biomolecules that result in inactivation since various plasma species, e.g. ions, reactive radicals, and UV/VUV photons may all contribute to deactivation. The present collaborative research projects involve an interdisciplinary team of investigators at University of Maryland, College Park (UMD), and University of California, Berkeley (UCB). The work is aimed at obtaining a scientific understanding of ion, energetic photon, and reactive neutral initiated processes and changes of surface/near-surface properties of the treated biological entities and correlation with altered biological function. Additionally, theoretical models which will assist with interpretation of experimental observations and formulation of a consistent framework will be developed based upon molecular dynamics simulations. The **Project Participants** include at

a) **UMD, College Park**, Profs. G. S. Oehrlein and J. Seog, and graduate student E. Bartis and undergraduate student S. Shachar (summer 2011) and
b) **UC Berkeley**, Profs. D. Graves and J.-W. Chu, along with post-doc N. Ning and graduate student T.-Y. Chung.

The collaboration has produced promising results during the first year of performance. We have had monthly phone conferences of all the participants to review progress and plans. During the conferences, the students/post-doc appointed on the project present the status of their work. We have selected lipopolysaccharides (LPS), a main component of the outer membrane of gram-negative bacteria that are notoriously difficult to remove from surfaces by conventional methods such as autoclaving and toxic washes without damaging the material from which they are being removed [3], as one material to investigate. In addition, studies with lipid A have been performed at UCB.

Plasma Processing and Materials Characterization at UMD

At UMD, graduate student Elliot Bartis prepared samples of LPS from E. coli O111:B4 spotted on Si chips and subsequently processed them in an inductively-coupled plasma. The plasma-treated LPS was characterized by x-ray photoelectron spectroscopy (XPS), *ex situ* ellipsometry, atomic force microscopy (AFM), and *in situ* real-time ellipsometry.

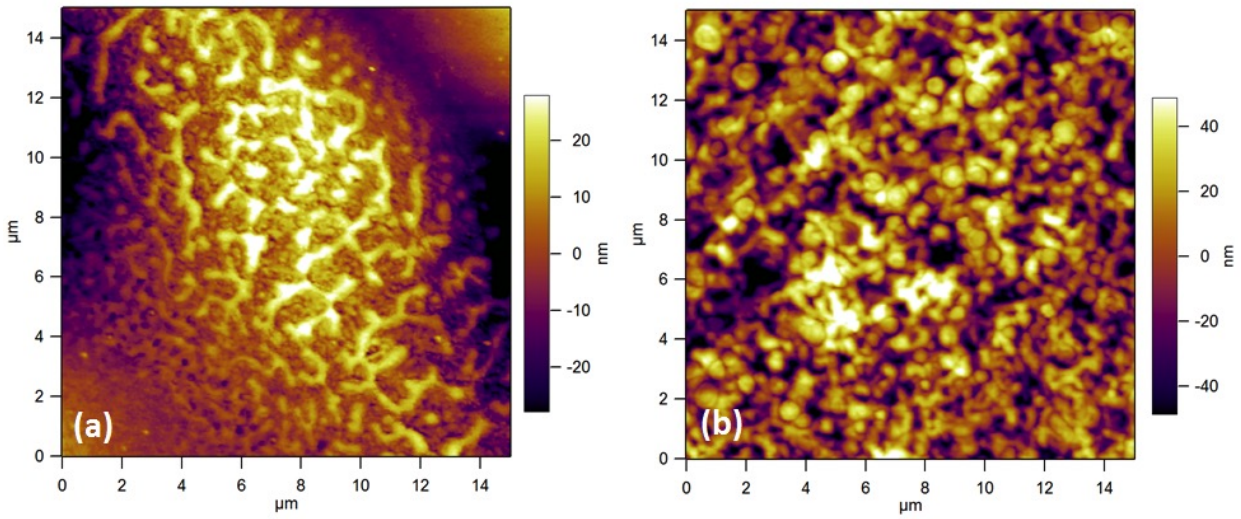

Figure 1: Atomic force microscopy topographic images of untreated surfaces prepared by spotting LPS on Si substrates. In (a) we see a networked structure while in (b) we see more spherical features. AFM images show that the surface is very non-uniform and that feature sizes can vary by tens of nanometers. AFM images were measured using AC mode in air.

LPS consists of a polysaccharide chain and lipid A, the latter of which triggers an innate immune response when it forms a complex with lipopolysaccharide binding protein (LBP). Plasma-induced modifications that disrupt the formation of this complex would indicate that deactivation has occurred. Lipid A consists of a *β*-1,6-linked D-glucosamine disaccharide carrying three phosphate groups and attached to aliphatic chains by ester and amide linkages. Some of the ester and amide linkages are linked to additional aliphatic chains by ester and ether linkages. Previous studies have found that adding H_2 to an Ar discharge leads to a reduction of infrared bands originating from the aliphatic chains of lipid A, namely C-H_x stretching, C-O, and amide bands [4]. By using Ar/H_2 mixtures, we can distinguish the roles of physical sputtering, which would dominate in the Ar discharge, and chemical attack by H-atoms, which would dominate in the H_2 discharge. In addition, we can examine the role of UV/VUV photons generated in the different discharges. In this **progress report**, we present an update on the project, including results of LPS modifications in pure Ar, 20% H_2 in Ar, and pure H_2 discharges. These treatments were all conducted without an RF bias; the ion energy is estimated at ~20eV.

Various approaches toward effective sample preparation have been investigated. LPS dissolved in distilled water was spotted on Si chips and left to dry under a standard flow hood. This technique caused the majority of the solution to aggregate in a corner of the sample. Similar results were found for drying the sample in a vacuum oven. Samples were also prepared by spin coating and dip coating on Si and amine-coated Si surfaces. The amine-coated surfaces were prepared by both plasma deposition using a N_2/H_2 gas mixture as well as immersing Si chips in (3-aminopropyl)triethoxysilane. These techniques left an extremely thin

% H in Ar	ER at start	ER at (i)	ER at (ii)	C 1s	O 1s	N 1s
0	0.7 nm/s	0.33 nm/s	0.2 nm/s	Less C-C/C-H, C-O, more amide	Less Cx-Oy & phosphate	largest increase
20	0.5 nm/s	n/a	n/a	Less C-C/C-H (surface), C-O	Less Cx-Oy & phosphate	small increase at surface
100	0.4 nm/s	0.18 nm/s	0.08 nm/s	Less C-C/C-H (surface), C-O	Less Cx-Oy & phosphate	small increase in bulk

Table 1: Measured etch rates corresponding to the data shown in Fig. 2b at (i) and (ii) as well as chemical changes extracted from XPS analysis.

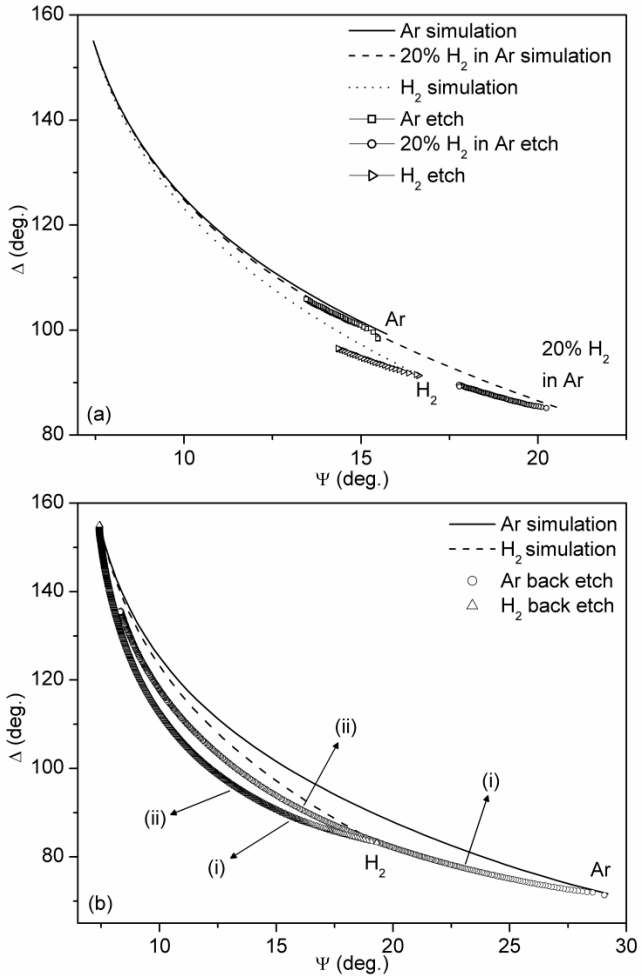

Figure 2: Ψ-Δ plots of LPS-spotted samples treated by pure Ar, 20% H_2 in Ar, and pure H_2. In (a), solid, dashed, and dotted lines represent simulations of the initial properties of the films for pure Ar, 20% H_2 in Ar, and pure H_2, respectively. In (b), back etched samples show a decreased etch rate as well as densification with increasing treatment time when compared to a simulation based on the films' initial properties. (i) and (ii) refer to etch rates presented in Table 1. Ar and 20% H_2 in Ar discharges were generated using a 300 W source power, 10 mTorr pressure, 50 SCCM gas flow, and no rf bias. H_2 discharges were generated using a 600 W and 500 W source power for the 12s and back etched samples, respectively, 30 mTorr pressure, 50 SCCM gas flow, and no rf bias.

(~5-10 nm) layer of LPS on the surface. AFM images of the spin coated samples showed a non-uniformly covered surface with large amounts of Si exposed. It was found that the most uniformly thick films were created by spotting LPS solution on a Si chip and allowing the sample to dry in a covered petri dish in an oven at 65°C. AFM images of surface morphologies observed on our two exemplary samples are shown in Fig. 1. We hypothesize that the variety of possible surface morphologies could influence the initial optical properties of the films as measured by ellipsometry.

We examined changes in optical properties and etch rates by utilizing *in situ* real time ellipsometry. Fig 2 (a) shows short etches for pure Ar, 20% H_2 in Ar, and pure H_2. Along with the measured data, simulations are shown based on the initial properties of each film are shown assuming constant composition. The observation that the simulated trajectories do not overlap with our experimental data indicates that the films have different initial optical properties. This is likely to be related to the heterogeneous structures of LPS film observed in AFM images but further investigations are need to confirm it. We performed treatment of our samples in pure Ar and pure H_2 discharges until there were no longer any changes in the Ψ-Δ curve. These treatments induce etching of the material, which is referred to as a back etch and is shown in Fig. 2 (b). The etch rates at the start of the treatment and at points (i) and (ii) in Fig. 2 (b) are shown in Table 1. This decrease in etch rate suggests that easily-removed species are

removed during the beginning of the treatment. In terms of deactivation, this could imply that relatively short exposures are enough to modify biomolecules at the surface of the film and decrease their pyrogenicity. Fig. 2 (a) shows a 12s etch of 20% H_2 in Ar. The etch rate here is approximately 0.5 nm/s. This decrease compared to the pure Ar case is likely due to a decrease in plasma density as H_2 is added to the discharge. Also observed in this treatment is an increased etch rate between t = 5s and t = 10s (~2x). The change of etch rate in a short time period could result from easily-removed groups being exposed after the near-surface lipid A layer is removed.

The increased difference between simulated curves and experimental data in Figures 2(a) and (b) also show that a large amount of densification occurs over the treatment time. Similarly to the decrease in etch rate, this densification could result from difficult-to-remove species, which have dangling bonds that are capable of crosslinking. However, the degree of densification seemed to vary as seen in Fig. 2 (a) for the Ar treatment, where very little densification occurs during the treatment.

XPS is a useful tool for studying surfaces as the technique probes only the first 10nm into the sample. XPS analysis of untreated samples shows that the near surface is O-deficient compared to the bulk of the sample, which suggests that lipid A's aliphatic chains organize at the air-water interface as the sample dries. This lipid A near-surface layer has a depth of approximately 3 nm into the film. As this is comparable to the electron inelastic mean free path through the film, approximately 63% of the signal comes from lipid A at normal electron emission while nearly all of the signal comes from lipid A for angle resolved XPS. Thus, this lipid A near-surface layer is greatly attenuating any signal coming from below the surface. If the surface layer is removed, then the signal from the polysaccharide portion of LPS should be enhanced, which would result in a significant increase in O and N signals. In all plasma treatments, more than 5 nm of material was removed during the treatment as measured by ellipsometry.

XPS difference spectra (treated-untreated) collected at normal electron emission of the C 1s, N 1s, and O 1s regions are shown in Fig. 3. C 1s difference plots show strong differences between the Ar-treated samples and the samples with H_2 in the discharge. These differences are mainly seen in the higher binding energy components resulting from O-C-O/amide groups

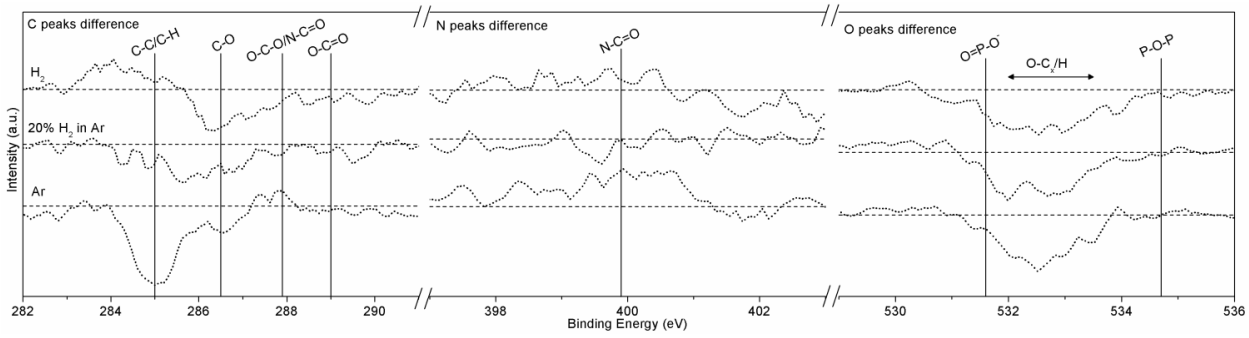

Figure 3: XPS difference spectra of C 1s, O 1s, and N 1s peaks after treatment with pure Ar, 20% H_2 in Ar, and pure H_2 taken at normal electron emission. In the carbon spectra, there is a decrease in C-C/C-H and increase in O-C-O/N-C=O peaks for pure Ar compared to the H_2-containing discharges. In the nitrogen spectra we see a larger increase in the N-C=O peak after the Ar treatment compared to H_2-containing discharges. In the oxygen spectra we see approximately equal decreases in the O 1s spectra corresponding to phosphate groups and O bonded to C or H. All discharges were generated using 150 W source power, 10 mTorr pressure, 50 SCCM gas flow, and no rf bias.

that are increased after Ar treatment but are decreased when H_2 is added to the plasma. N 1s difference plots show weak, but observable changes corresponding to amide structures that are found in lipid A portion as well as the N-acetyl-glucosamine and N-acetyl galactosamine residues present in the polysaccharide portion. For the pure Ar discharge, we see an increased amide signal compared to when H_2 is added to the discharge. In all plasma chemistries, there is a decrease in O corresponding to C-O, OH, and ester groups (ester group changed barely in Ar treatment). The removed O results from removal of -OH groups, and C-O bonds in the polysaccharide. However, as the difference plots indicate, O is also removed from the phosphate groups on lipid A in the form of $O=P-O^-$.

Angle resolved XPS analysis (results are not shown due to space limitations) was used to obtain chemical changes as a function of depth. We found that C-C/C-H groups are decreased in all cases close to the surface. As the largest changes occur at low electron emission angles, the decrease after treatment is mainly due to the removal of aliphatic chain in lipid A portion. Adding H_2 to the discharge also decreases the amount of C-O bonds in the molecule compared to pure Ar. This decrease could result from modification/breaking of the ether bonds in lipid A and the polysaccharide chains. With the pure H_2 discharge, we see a decrease in O at low electron emission angles that is not seen in Ar containing discharges. Near the surface, the N/C ratio increases by ~84% for the Ar treatment compared to the untreated sample. When adding H_2 to the discharge, the increase in N/C decreased strongly. For 20% H_2 addition to Ar and pure H_2, the N/C ratio at the surface increases by 44% and 21%, respectively.

The increase of amide and ester groups for the Ar treatment compared to H_2 containing discharges could suggest that Ar does not as preferentially remove O or N over C compared to H_2. The decrease in C-C/C-H groups near the surface could correspond to modification or removal of the aliphatic chains present on lipid A as well as the polysaccharide chain. The additional O-loss near the surface for the pure H_2 discharges could suggest that adding H_2 enhances the removal of O at the surface compared to Ar. As noted above, it is expected for the N signal to increase due to less attenuation by the near-surface lipid A. The fact that the N/C ratio increases less as more H_2 is added to the discharge could indicate that the presence of H_2 more effectively removes amide groups. This is consistent with Kylian's FT-IR results where there is a decreased signal from amides when H_2 is added to the discharge. The removal of amide groups on lipid A could result in a major chemical/structural modification of lipid A as the amide groups link the disaccharide backbone to the aliphatic chains. Kylian et al. have also shown that the presence of atomic hydrogen in a microwave discharge causes a reduction of C=O bands as measured by FT-IR as well as a modification of phosphoryl groups as measured by ToF-SIMS. Modification of the phosphoryl groups is important because it has been shown that monophosphoryl lipid A is considered non-toxic compared to diphosphoryl lipid A [4].

It is likely that UV/VUV effects become more important as H_2 is added to the plasma discharge. Complementary VUV beam studies performed at UCB are consistent with our XPS results. FT-IR and electrospray ionization mass spectrometry spectra show decreased amide, ester, phosphate, and aliphatic carbon signals after beam exposure.

At UMD, our next steps include the following: To examine the role of vacuum UV (VUV)-induced photolysis in these chemical changes, we plan to use an VUV optical filter approach to probe VUV-induced LPS surface modifications in real time by in-situ ellipsometry during LTP processing while protecting the material against ion bombardment, along with additional

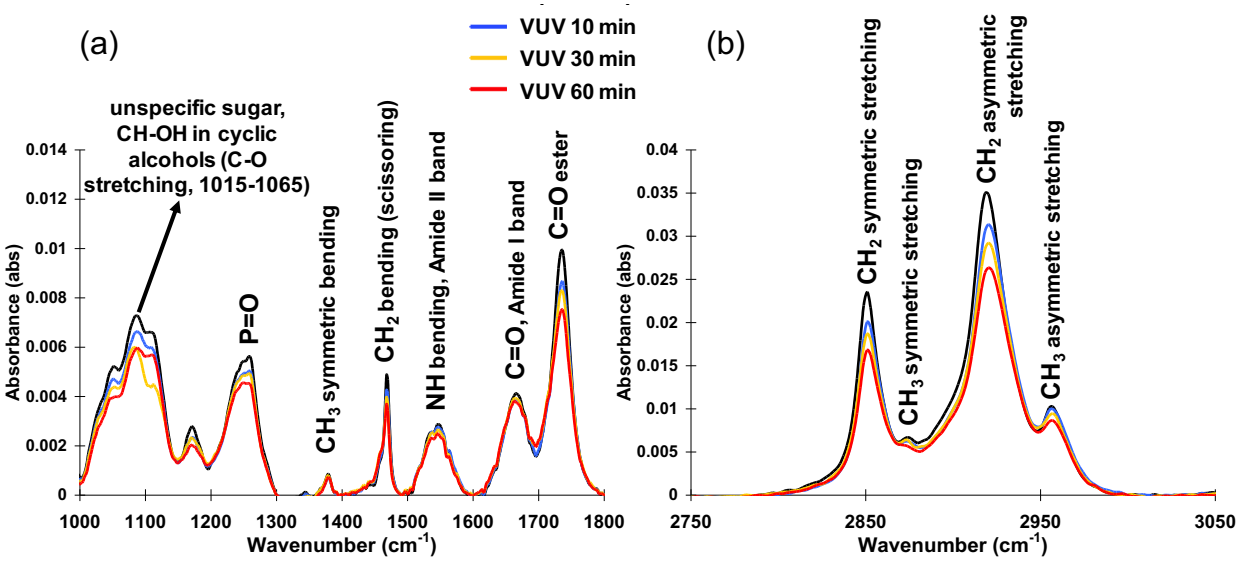

Figure 4. Transmission FTIR spectra of lipid A after exposure to VUV photons with different exposure time. The photon flux was of 1.34×10^{14} photons/cm^2·sec. (a) 1000-1800 cm^{-1} (b) 2750-3050 cm^{-1}.

surface chemical characterization. Results of biological assay tests conducted using an enzyme-linked immunosorbent assay with lipopolysaccharide binding prot ein will also be performed. Additionally, we plan to perform complementary studies with lipid A to compare directly the results of the UMD work with the results of the UCB beam studies.

Vacuum Beam Studies at UCB

At UCB, we used a vacuum beam apparatus to study energetic beam effects on LPS and/or lipid A. This study complements the work performed at UMD with plasma exposure. Initial efforts in year 1 have focused on sample preparation, the effects of sample exposure using 147 nm photons, and pre- and post-exposure sample characterization. In the interests of brevity, we focus here on major results and do not list all of the initial studies. We note that actual plasma exposure will have a spectrum of UV and VUV impacting the sample, but by using a single wavelength at known fluxes and fluences (or doses), it will be possible to understand the role of photons alone. Initial investigations showed that the effects of photon exposure of LPS films are difficult to interpret using transmission Fourier transform infrared (FT-IR) spectroscopy and it was therefore decided to focus on the simpler lipid A samples. It is generally recognized that lipid A is the primary component of LPS that leads to pyrogenicity, so

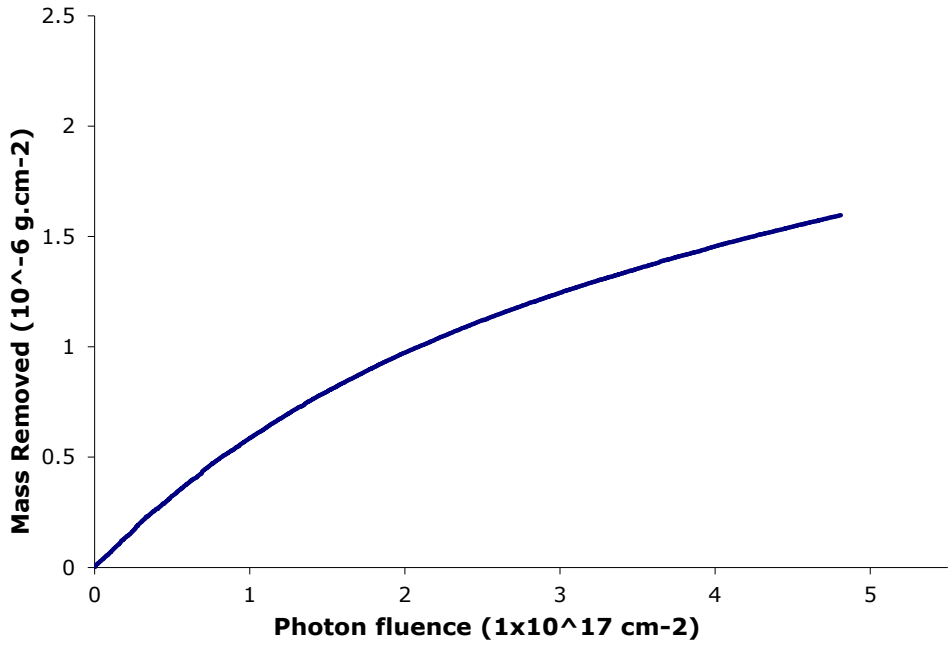

Figure 5. In-situ mass removal of lipid A by VUV exposure. The presented data is an average of three independent measurements.

this lipid A focus does not limit the generality of the investigation. Lipid A was dissolved in a solution of chloroform, methanol, and water (composition ratio of 74:23:3, respectively) and spotted on ~ 1cm ×1cm silicon substrates and

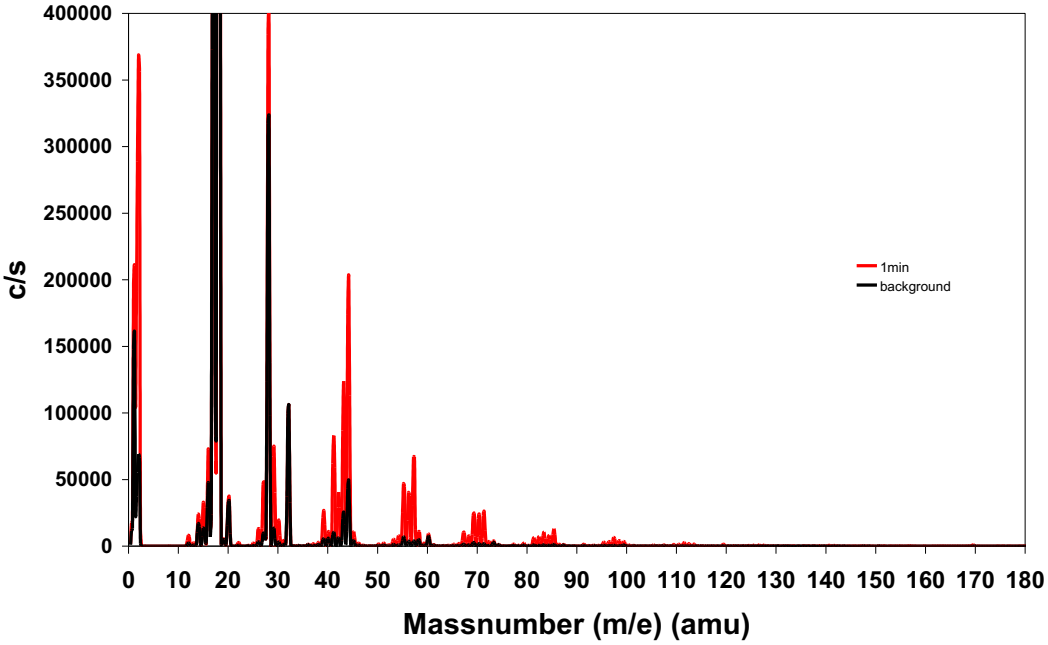

Figure 6. *In-situ* mass spectrometry measurement of lipid A after ~8×10^{15} photons/cm^2 VUV exposure.

placed in the chamber for exposure. After vacuum ultraviolet (VUV) photon exposure (with ph oton flux ~1.3 x 10^{14} photons $s^{-1}cm^{-2}$), loss of CH_2/CH_3, C=O ester, and P=O absorption peaks were observed by *ex-situ* FT-IR spectroscopy, but the C=O amide absorption peak was only mildly affected (Figure 4). Experiments with samples on an *in-situ* quartz crystal microbalance (measuring mass loss from the sample) confirmed the expected VUV-induced mass loss of exposed lipid A (Figure 5). (The maximum photon dose of about 5 x 10^{17} cm^{-2} on the plot in Fig. 5 corresponds to the 60 minute exposure in Fig. 4 and might represent several tens of seconds of actual plasma exposure, depending on the plasma photon generation rate.)

Monitoring the low molecular weight photolysis products (< 300 amu) from lipid A films by *in-situ* mass spectrometry, we observed cracking patterns similar to those of alkanes/alkenes with a carbon number ~11-13 (Figure 6). Exposed lipid A films were re-suspended in the solution noted above and analyzed by electrospray ionization (ESI) time-of-flight mass spectrometry (ToF MS) in negative ion mode. ESI MS is a powerful tool to measure large molecular weight biological samples with minimal cracking, but negative ion and positive ion modes typically give complementary mass spectra. Our lipid A sample was obtained commercially, and was prepared from *Salmonella enterica* serotype minnesota Re 595. The ESI MS measurement showed that the as-received pristine lipid A sample includes various non-stoichiometric substitutions, i.e. mass peaks at 1796.3, 1919.3, 1927.3, 2050.3, 2157.5, and 2288.5 (figure not shown). We observed the signals of intact lipid A molecules decrease with increasing VUV exposure time (Figure 7). Other VUV-photolyzed fragments will be further examined with the ESI MS in positive ion mode to show complementary sample photolysis components.

The results to date suggest that VUV photons remove intact lipid A molecules, break phosphate groups and ester linkages leading to desorption of acyl chains. It is known that the endotoxicity of lipid A is primarily determined by the number and length of acyl chains as well as the phosphorylation state and the disaccharide backbone. The present results

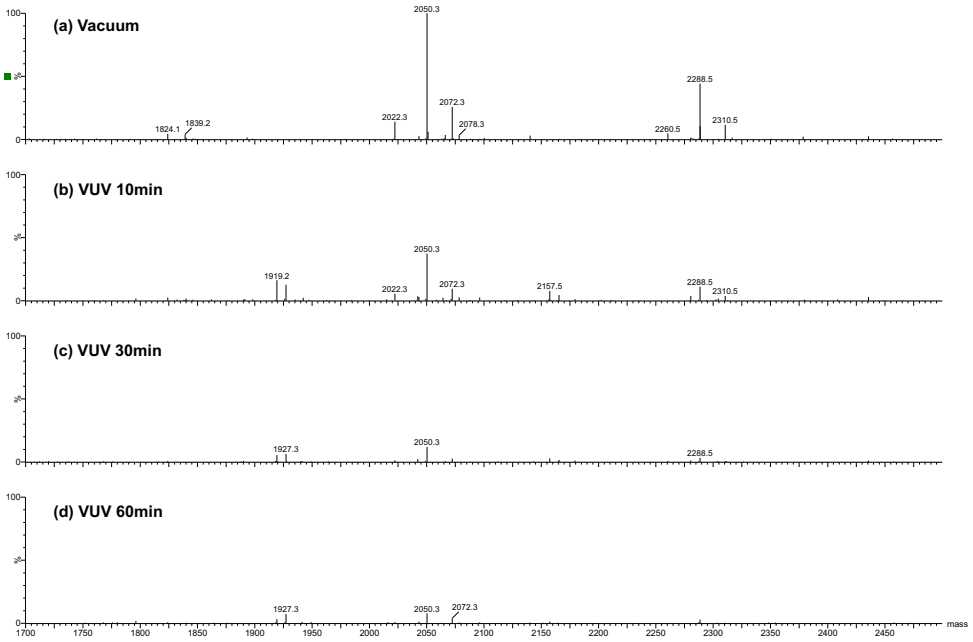

Figure 7. ESI mass spectrometry measurements of lipid A (a) vacuum 60 min; (b) VUV 10 min; (c) VUV 30min; and (d) VUV 60min. Spectra are scaled to *m/z* = 2050 ion in (a).

therefore are consistent with the conclusion that plasma-generated VUV photolysis reduces the endotoxicity of lipid A.

XPS analysis performed on LPS samples prepared at UMD suggest that lipid A aliphatic chains segregate to the sample surface. After all plasma treatments, C-C/C-H groups are observd to decrease at the near-surface indicating the removal of these aliphatic chains. Additional O loss near the surface is observed after adding H_2 to the argon discharge. As VUV emission is known to be especially intense in H_2-containing plasmas, VUV is suspected to play an important role in lipid A/LPS modification in H_2-containing discharges. This is consistent with our observations as noted above.

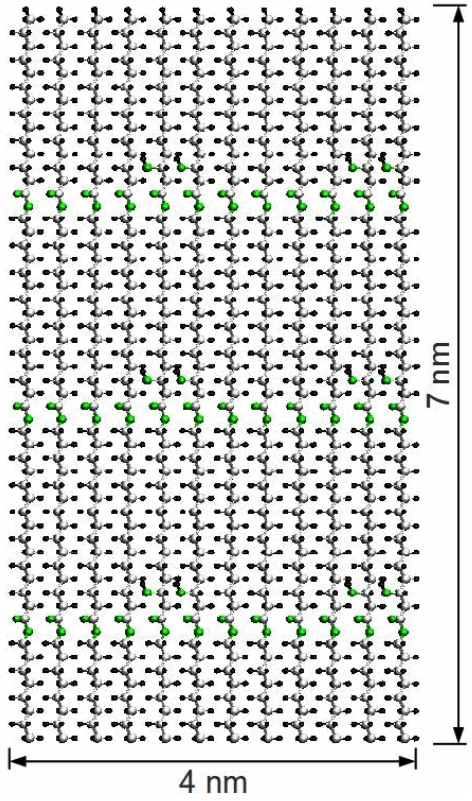

Figure 8. Side view image of the model lipid A acyl chain film. The silver balls are C; black balls are H and green balls are O.

In future work, we plan to directly determine sample pyrogenicity (i.e. toxicity) by

using a human 'whole blood' test, which is based on the measurement of cytokine release from leukocytes by an enzyme-linked immunosorbent assay (ELISA). We will also examine LPS samples to compare directly with the UMD results. A recently added radical source will allow sample exposure with beams of H, O and NH_x radicals, among others.

Molecular Dynamics Simulations at UCB

The role of the molecular dynamic simulations is to help interpret vacuum beam and plasma exposure measurements to provide insights into deactivation mechanisms. In order to understand the effects of Ar/H_2 plasmas on lipid A, the preliminary molecular dynamics (MD) simulations study is focused on the interaction of Ar^+, Ar^+/H and Ar^+/O with model acyl chains of lipid A (Figure 8). Here, w e report on the initial results of the effects of Ar ion physical sputtering only.

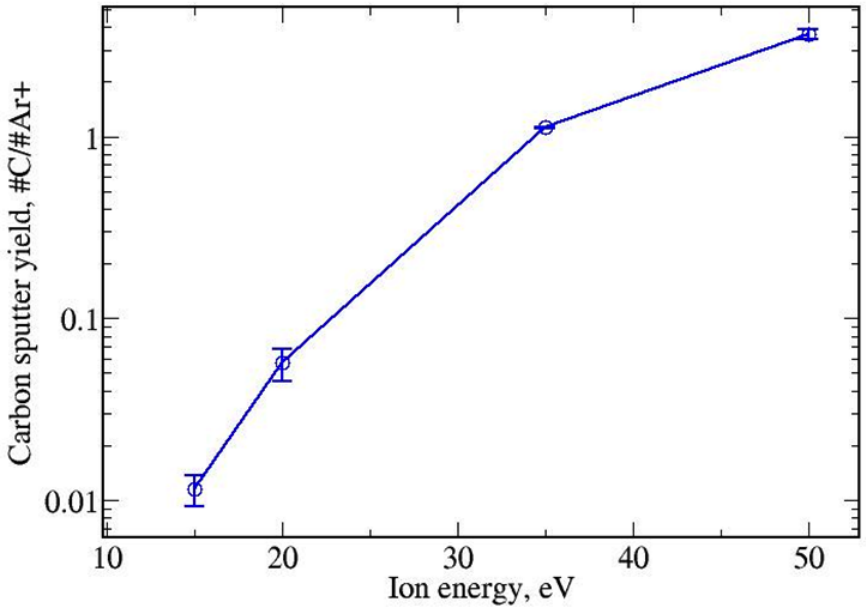

Figure 9. Carbon sputtering yield as a function of Ar^+ energy at normal incidence, each point representing an average of over 3000 simulated ion impacts, or an ion fluence of $4 \times 10^{16} cm^{-2}$.

We constructed the mode l acyl chains to be initially aligned vertically, as Figure 8 illustrates. The model film dimensions are 3x4x7 nm and its mass density is 0.8 g/cm^3. The bottom ~2 nm of the simulated film is kept rigid in order to avoid transition in space during the collision. The film temperature is initially 300 K; the film is cooled back to 300 K after each trajectory simulation. Each trajectory is followed for 1ps (10^{-12} s). The studied ion energy ranges from 15 to 50 eV. Total ion fluence in the simulation is $4x10^{16} cm^{-2}$, corresponding to about 10 s exposure of an ion current of 1 mA/cm^2.

As shown in Figure 9, the energy threshold of physical sputtering by argon ion bombardment is ~15 eV. The O-to-C and H-to-C ratios of the film treated by argon ion bombardment are barely changed with increasing ion energy. Just above the physical sputtering threshold, (~20 eV), the major carbon sputtered species are molecules containing 11-2 0 carbon atoms. For the higher ion energy cases (35 and 50 eV), small molecules became the more dominant products. We also observe the ejection of some larger fragment molecules, which is probably due to the deeper penetration depth associated with the higher ion energy.

Future MD work will focus on simulating ion/radical interaction with the model acyl chain of LPS endotoxin lipid A, as well as the effects of photons on acyl chain removal. These predictions can be directly compared with the current and planned vacuum beam exposures, and eventually to the plasma studies as well.

[1]A. von Keudell et al., Plasma Process. Polym. **7**, 327 (2010)
[2]H. Rauscher et al., Chem. Phys. Chem. **11**, 1382 (2010)
[3] E. T. Rietschel et al., FASEB J. **8**, 217 (1994)
[4]O. Kylian et al., Plasma Process. Polym. **5**, 26 (2008)

Year 2 Progress Report, May 2012: Activities and Findings

Plasma Processing and Materials Characterization at UMD

In year 2, we focused on isolating the effects of plasma-generated VUV and plasma-generated radicals from inert (Ar) and reactive (H_2) plasmas. We also developed an enzyme-linked immunosorbent assay to measure the biological activity after plasma exposure. VUV-only experiments were performed by covering the sample with a MgF_2 filter, which physically prevents ions and neutrals from reaching the sample and only transmits wavelengths above 112 nm, which includes the 121 nm Lyman α line photons from atomic hydrogen. Radical-only treatments were performed by employing a gap structure that rests on top of the sample. The high aspect ratio of the gap structure allows for the diffusion of neutrals while ions are effectively removed by collisions with surfaces.

We studied the deactivation of biotinylated-LPS (bLPS) using an enzyme-linked immunosorbent assay (ELISA). ELISA is an extremely sensitive technique that can detect antigen concentrations in the ng/mL range. The presence of an antigen causes a quantifiable color change in the well whose measurable absorbance relates to the amount of antigen in the sample. Direct, UV/VUV-only, and radical-only exposures all caused some degree of deactivation. As bLPS forms a very thin film in the well, direct exposures caused a significant degree of deactivation with only small differences between pure Ar and pure H_2 discharges. For UV/VUV-only treatments, Ar discharges do not emit UV/VUV photons at wavelengths greater than the cut-off wavelength of the MgF_2 filter, so no deactivation was observed. H_2 plasma emits high energy photons that cause a small degree of deactivation. This deactivation is low because UV/VUV photons can penetrate as deep as 200 nm into polymer samples, so the probability of a photon interacting with the adsorbed layer in the well plate is low.

Radical-only treatments employing a gap structure showed clear evidence for deactivation. The gap structure sits 1.4 mm above the sample and allows for one-dimensional diffusion of neutrals and prevents ion bombardment of the surface because plasma is not produced within the gap. Additionally, ions that diffuse into the gap are effectively quenched by collisions with surfaces. Figure 1 shows the normalized absorbance as a function of the aspect ratio, which is determined by the distance from the edge of the gap, for different treatment times. The effect of the aspect ratio is clearly observed in the deactivation as less deactivation occurs for higher aspect ratios. For Ar, we see an absorbance increase for aspect ratios greater than 8. It is possible that the deactivation seen close to the edge of the structure is caused by Ar metastables. The sharp increase shows that diffused Ar neutrals are not effective in deactivating bLPS. In contrast, plasma-generated H radicals are very reactive with the surface and cause deactivation even at high aspect ratios. The effect of diffusion is also observed as less deactivation occurs for higher aspect ratios. As the treatment time is increased, there is clear evidence for increased deactivation as more reactive neutrals can diffuse to the surface.

XPS difference spectra (UV/VUV-treated – untreated) of lipid A films collected at normal electron emission of the C 1s, N 1s, O 1s, and P 2p regions are shown in Fig. 2. As Ar does not emit high energy photons capable of modifying or etching the samples, we do not see dramatic changes in the spectra or chemical composition of the films. We observe a small decrease in C-C/C-H bonding after treatment, which likely results from small amounts of chamber contamination, i.e. oxygen from the quartz coupling window. The high energy photons generated in H_2 plasmas have a large impact on the C

1s spectra. We see a clear decrease in the higher binding energy components resulting from C-O, C=O/N-C=O, and O-C=O groups. The aliphatic chains on lipid A are connected to the disaccharide backbone by N-C=O and O-C=O linkages. The removal of these groups suggests that these aliphatic chains are being removed. The length and number of these aliphatic chains contributes to the toxicity of lipid A, so if they are removed or modified, the bioactivity is reduced. The C 1s difference spectrum also shows an increase in C-C/C-H groups. This indicates that the disaccharide backbone has been modified by the removal of –OH groups, which is confirmed by the decrease in C-O bonding. There are no changes observed in the P 2p and N 1s spectra, indicating that the N and P moieties that remain in the film after treatment are not modified by the treatment. In the O 1s, we see that UV/VUV photons cause a slight shift toward lower binding energy, which is consistent with the removal of the high binding energy groups observed in the C 1s spectrum. The chemical composition of the films was also studied. As expected, minimal changes occur after the Ar treatment.

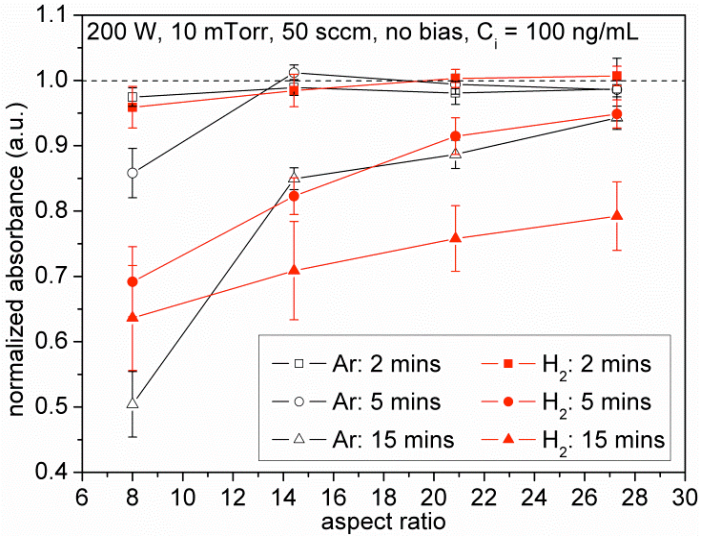

Figure 1: An enzyme linked immunosorbent assay was utilized to determine the decrease in biological activity after radical-only treatments employing a gap structure in Ar and H_2 plasma. Biological activity decreases at high aspect ratios only for H_2 plasmas, which indicates that atomic H reacts with the surface while inert Ar atoms do not. Discharges were generated with 200 W source power, 10 mTorr operating pressure, 50 sccm gas flow rate, and without external bias.

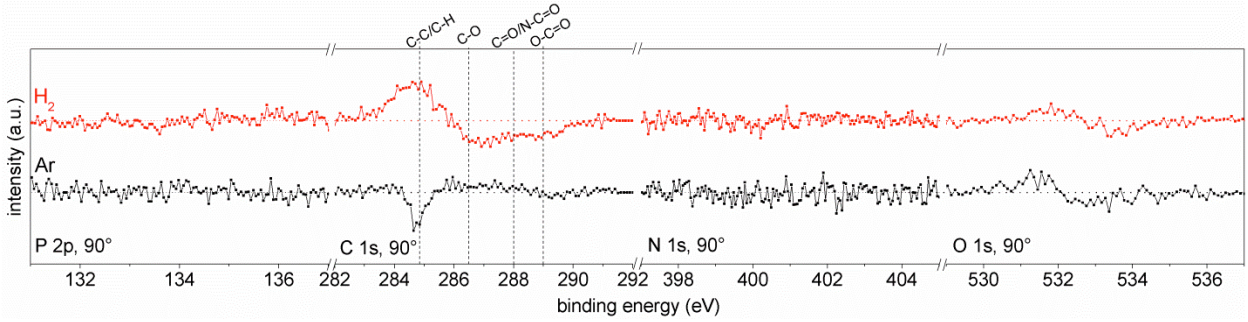

Figure 2: XPS difference spectrum of P 2p, C 1s, N 1s, and O 1s after treatment with radiation generated by pure Ar and H_2 plasmas taken at normal electron emission. In the P 2p and N 1s spectra, we do not see any change in the chemical state. In the C 1s, Ar discharges cause a small decrease in C-C/C-H moieties that likely results from impurities in the chamber. For H_2 discharges, we see a strong decrease in high binding energy groups corresponding to C-O, C=O/N-C=O and O-C=O and an increase in C-C/C-H groups, which indicates that oxygen is being preferentially removed from the molecule, leaving a C-rich film. In the O 1s, we see a shift toward lower binding energies after treatment which is consistent with the decrease in high binding energy groups seen in the C

1s. All discharges were generated at 30 mTorr pressure, 50 sccm gas flow rate, and without rf bias. Ar and H_2 discharges were generated at 300 W and 600 W, respectively.

UV/VUV photons from the H_2 treatment cause the O content to decrease from ~19% to ~10%. This decrease is complemented by an equal increase in C content from ~78% to 87%. Oxygen from the phosphate groups does not seem to be affected, as we do not observe a chemical shift in the P 2p difference spectrum.

We conclude that the dominant effect of H_2 plasma-generated UV/VUV radiation is to remove carbon-bound oxygen from the biomolecule. Complementary experiments were conducted on LPS films. LPS films have a significantly higher amount of N and C-O groups present due to the O-chain. The dominant effect observed in the C 1s is a decrease in C-O groups, which is supported by a reduction in the O-content in the film.

Real-time *in situ* ellipsometry was used to study the effects of VUV/UV radiation from pure Ar, 20% H_2 in Ar, and pure H_2 plasma chemistries on LPS films. Figure 3 demonstrates that adding H_2 to the discharge increases the etch rate. With pure Ar, minimal etching occurs. This etching is likely due to small chamber contaminations. When the sample is treated with a pure H_2 plasma, we observe a nearly 20% decrease in the sample thickness in 120 seconds of treatment. After the first 120 seconds, the etch rate significantly slows down. As a significant fraction of the film thickness remains, we can conclude that there are a limited number of components that can be removed by UV/VUV radiation.

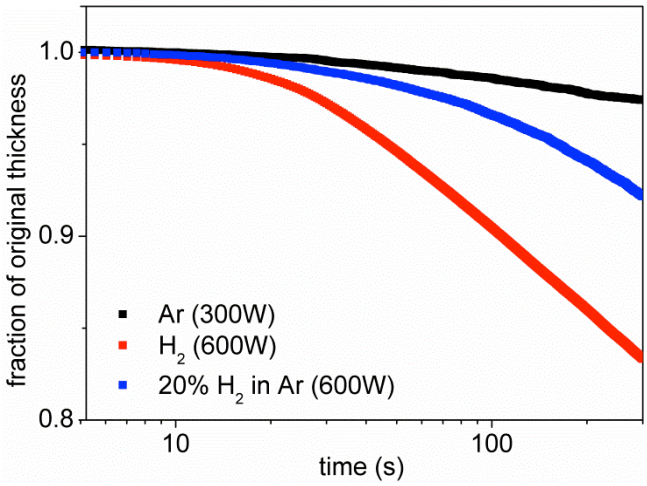

Figure 3: Real-time *in situ* ellipsometry shows that the VUV/UV photons from H_2 containing discharges effectively etch LPS films compared to Ar discharges. Pure Ar and 20% H_2 in Ar discharges were generated using 300 W source power, 30 mTorr pressure, 100 sccm gas flow rate, and no rf bias. H_2 containing discharges were generated using a 600 W source power, 30 mTorr pressure, 100 sccm gas flow rate, and no rf bias.

is

50

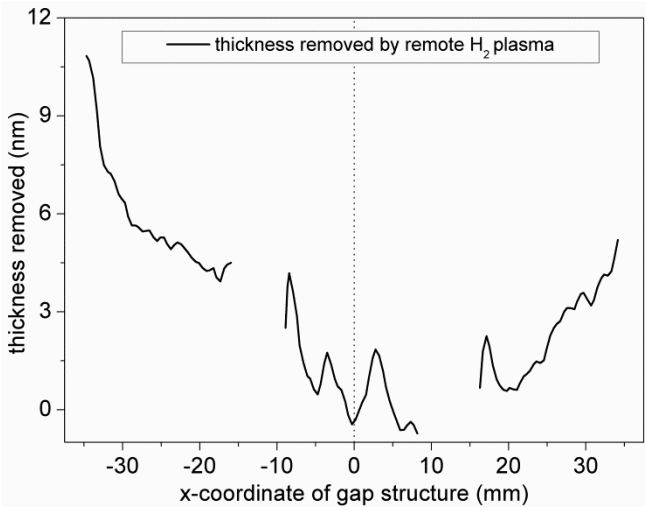

Figure 4: Thickness removed as a function of distance from the edge of the gap structure. As the edge of the gap structure is approached, the role of energetic species become more important and increased etching observed. The H_2 discharge was generated without external bias with 200 W source power, sccm gas flow rate, and 10 mTorr operating pressure.

We have also studied radical-only treatments by employing a gap structure, which isolates the role of neutrals. Ellipsometric measurements shown in Figure 4 demonstrate a clear decrease in etching as the center of the gap structure is approached. Furthermore, ellipsometry confirms that H atoms do not cause significant etching of our materials as less than 2 nm of material are removed in 15 minutes at the center of structure.

The ELISA experiments showed a clear decrease in biological activity for our samples exposed to radicals only. This is consistent with the idea that while etching does not play a large role with radical-only treatments, radical-induced surface modifications appear to be very important. In a 15 minute treatment under radical-only conditions, XPS analysis revealed a strong decrease in N and P and an increase in C. This suggests that H atoms are breaking amide bonds in the sample as well as volatilizing phosphorus. The C-rich film that remains on the surface is etch resistant, which is consistent with prior work which showed that amorphous carbon films cannot be etched effectively by H atoms under ambient conditions [1]. These results compare favorably with the complementary VUV/radical beam studies of lipid A performed at UCB and to be described next.

At UMD, our next steps include further study of the role of radicals in real-time by *in situ* ellipsometry and investigating the effects of atmospheric pressure plasma on LPS/lipid A films in a well-controlled environment.

Vacuum beam studies at UCB

In year 2, we have focused on using a thermal radical source to study radical-induced modification and chemical etching of lipid A films. The radical beam flux is characterized by threshold ionization mass spectrometry (TIMS). The typical oxygen radical flux is ~ 7.5×10^{13} oxygen/cm^2·s and the typical deuterium radical flux is ~ 4.6×10^{13} deuterium/cm^2·s. Also, considerable effort has been devoted to develop a reliable assay to quantify the endotoxic activity of lipid A after beam processes.

We have already shown in the year 1 report that VUV photons cause bulk modification to the penetration depth of lipid A film, ~ 200 nm. In contrast, radical exposures result in reactions at the surface of lipid A films, and thus the bulk properties are unaffected. Transmission FTIR measurements on radical-exposed samples show little change of absorption spectra (not shown). No enhanced bulk material removal is achieved by simultaneous exposure of the samples to radicals and VUV photons.

For oxygen radical exposure, the lipid A film etch yield measured by quartz crystal microbalance (QCM) is ~ 0.04 C/oxygen atom. This is in reasonable agreement with published Kapton (polyimide) etch yields.[2] Measurements of deuterium radical impact on lipid A film show a mass change within the uncertainty limit of our QCM setup, which is about 8.3×10^{-4} Hz/s. Using this value as an upper limit, we estimate a maximum etch yield of 0.02 C/deuterium atom. Our estimated maximum etch yield is in reasonable agreement with values obtained from hydrogen/deuterium radical erosion of amorphous hydrogenated carbon (a-C:H) films. [3, 4]

The radical-induced etch yield is relatively low compared to measurements made due to 147 nm VUV photons (initial etch yield is ~ 0.67 C/photon, and the steady state etch yield is ~ 0.15 C/photon). However, radical-induced chemical etching is expected to modify the surface of lipid A film. Time-of-flight secondary ion mass spectrometry (ToF-SIMS) is thus used to probe the film near-surface region (1~2 nm). Figure 5 shows the partial negative ion spectra of unprocessed lipid A film (*Salmonella minnesota* Re 595, 1mg/ml, 10 ul). Important fragments from intact lipid A molecules are observed and assigned in accordance with literature. [5-7]

Samples processed with VUV, O radicals, and D radicals were also analyzed by ToF-SIMS. The exposure time for each condition is 60 min, resulting in the species fluence of 4.9×10^{17} photons/cm^2, 2.7×10^{17} oxygen/cm^2, and 1.7×10^{17} deutrium/cm^2, respectively. Figure 6 shows the compiled results comparing the change of phosphates, pyrophosphates, and fatty acids, which are important factors governing the endotoxic activity of lipid A. VUV exposure results in removal of CH_2/CH_3, esters, and

phosphate groups from material bulk, which is also observed from surface sensitive SIMS measurements. Phosphates, pyrophosphates, and fatty acids peaks all decrease after 60 min of VUV exposures. In spite of low etch yield, O and D radical-exposed samples show significant modification at lipid A film surface. Phosphates, pyrophosphates, and fatty acid groups all decrease to an extent even lower than VUV-processed samples. Specifically, oxygen radical attacks the aliphatic moieties, which leaves little intact fatty acids on the film surface.

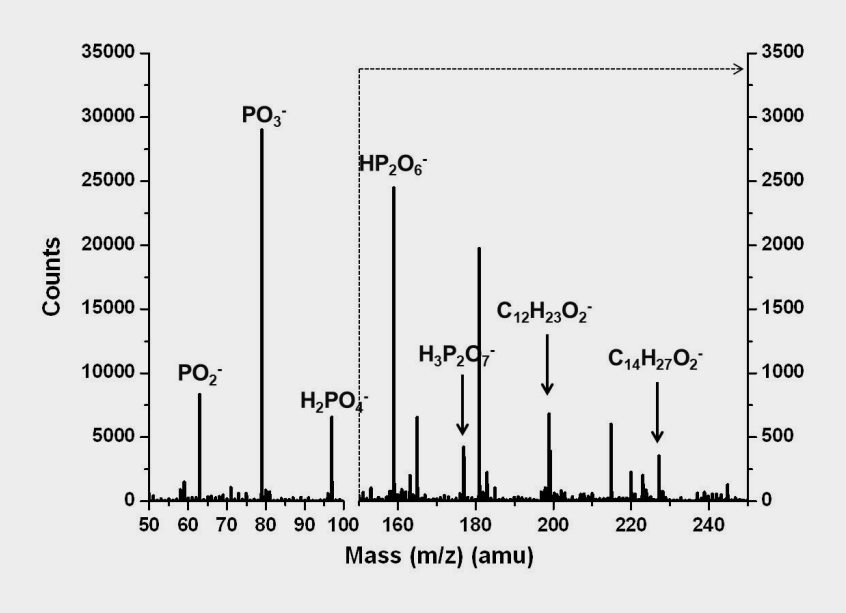

Figure 5. Partial negative ion ToF-SIMS spectra of unprocessed lipid A film. Note that the counts scale is different from 50-100 amu to 150-250 amu

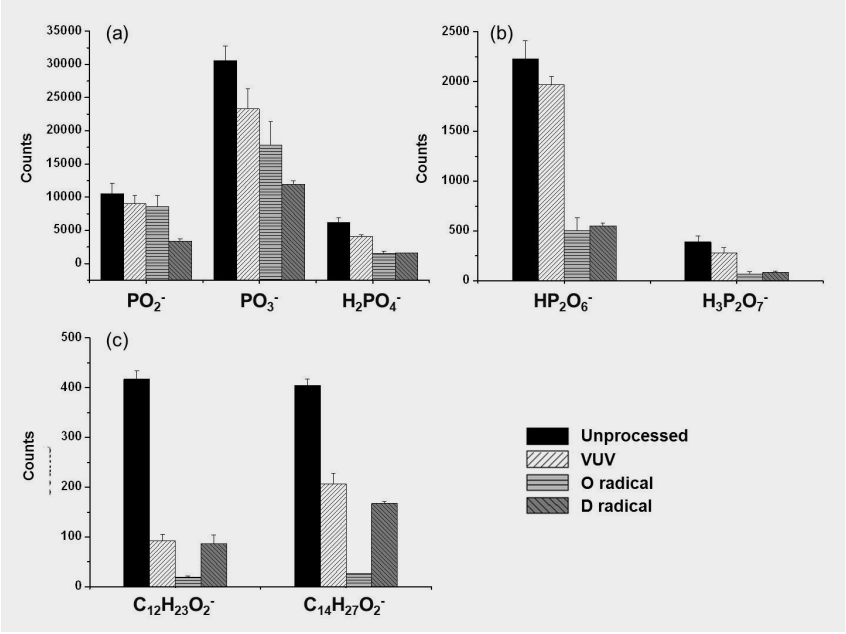

Figure 6. The change of characteristic ToF-SIMS peaks of (a) phosphates, (b) pyrophosphates, and (c) fatty acids with various exposure protocols.

Endotoxicity measurements are conducted by the human whole blood tests, utilizing the immune-stimulating nature of lipid A. Cells of mammalian immune system, such as monocytes and macrophages, can recognize LPS or lipid A through the Toll-like receptor 4 (TLR-4) and protein complex to initiate the secretion of a range of pro-inflammatory proteins, including interleukin-1β (IL-1β), IL-6, and tumor-necrosis factor-α (TNF-α). Thus, secreted interleukin concentration can be used as a gauge of endotoxic activity. We note that lipid A deposit is not readily soluble in blood. Thus, this assay mainly monitors the endotoxic activity of lipid A film surface.

Figure 7 shows the endotoxic activity of unprocessed and processed lipid A samples. We report results obtained from 4 healthy blood donors. For each donor, tests on serial unprocessed lipid A samples were performed, as shown in Figure 7a. UV/ozone-cleaved bare silicon doesn't activate IL-1β secretion. We note that the LPS/lipid A stimulation response from circulating leukocytes varies largely from individual to individual. As shown in Figure 7a, when the blood is stimulated with 2000 ng of lipid A, the difference between the highest responder (donor 4) and the lowest responder (donor 3) is about 15 folds. Wurfel et al reported that under the same stimulation condition, IL-1β concentration, measured from 102 normal subjects, could be differed by as many as 40 folds from the highest to the lowest responders.[8] Our result is within the range of variation reported by Wurfel et al.

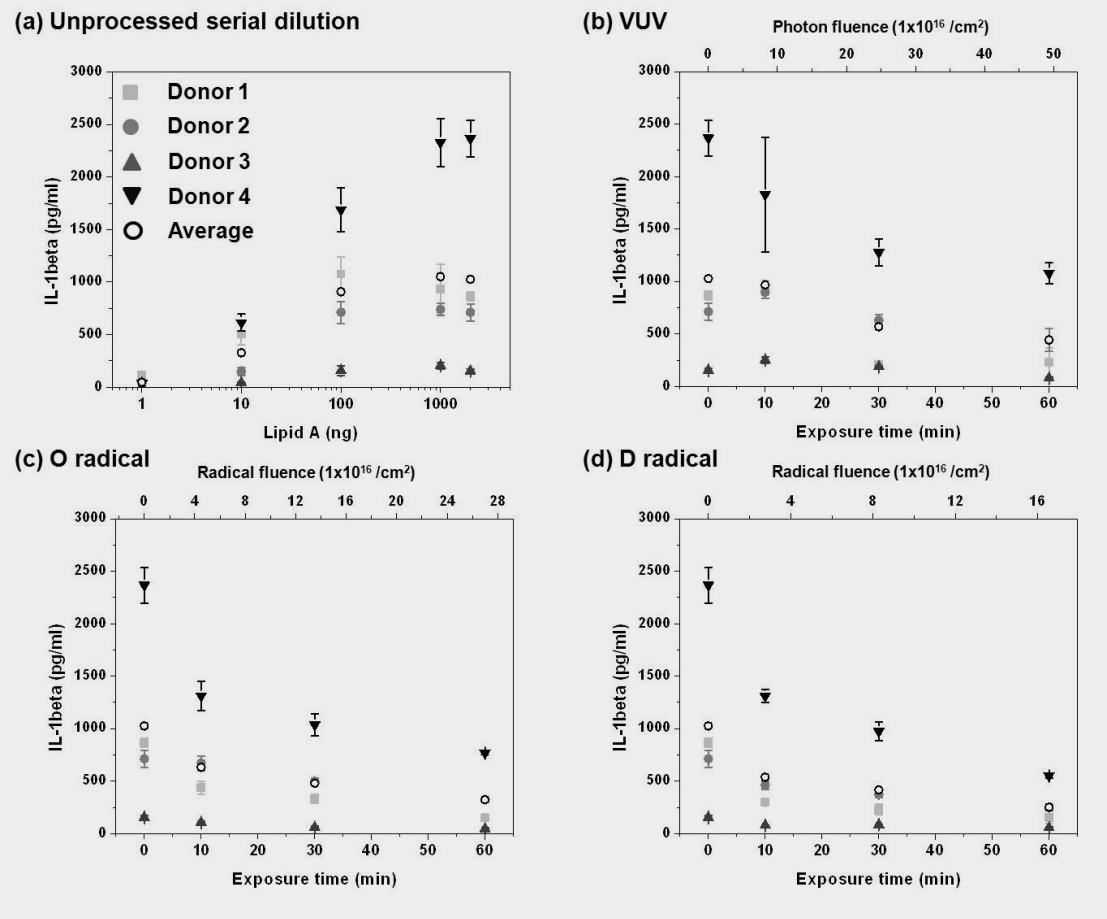

Figure 7. Endotoxic activity monitored by secreted IL-1β in human whole blood assay. Blood from 4 healthy donors were incubated with (a) unprocessed serial dilution, (b) VUV-processed, (c) O radical-processed, and (d) D radical-processed lipid A samples. The error bar for each data point stands for the standard deviation from 3 independent exposure samples tested with blood from the same donor.

The results of endotoxic activity change after beam exposures are shown in Figure 7b, 7c, and 7d for VUV, oxygen radical, and deuterium radical exposures, respectively. For oxygen and deuterium radical exposures, the average IL-1β concentration decreases with increasing exposure time. 60 minutes of oxygen or deuterium radical exposure (2.7×10^{17} oxygen/cm^2; 1.7×10^{17} deutrium/cm^2) results in average IL-1β concentration decreases to ~ 31% and ~25%, compared to unprocessed samples. After 60 minutes of VUV exposure (4.9×10^{17} photons/cm^2), average IL-1β concentration decreases to ~ 45% compared to unprocessed samples. We emphasize here that lipid A deposits are not readily soluble in human whole blood, and thus the human whole blood assay used in this study mainly monitors the change of lipid A film surface, where leukocytes contact the modified material. This surface sensitive assay suggests that under the same order of magnitude of total fluence, radicals have better efficacy in damaging the surface of lipid A deposits. ToF-SIMS measurements strongly support the results obtained from human whole blood assay, in which the entodoxic activity of lipid A is greatly reduced after radical exposures.

In summary, we have shown VUV-induced photolysis causes bulk modification of exposed lipid A film to the penetration depth of VUV photons (~ 200 nm). On the other hand, radicals mainly cause chemical etching and modification at the surface of lipid A film. Important structures governing the endotoxic activity of lipid A, e.g. the fatty acid chains and the phosphate groups, are greatly reduced after radical exposure. Although the radical mass etch yield is lower than that by VUV-induced photolysis, SIMS and human whole blood-based assay suggest radicals render a higher degree of modification at the film surface. Future work will include the role of low energy ions to fully understand the plasma effect on lipid A and other biomolecules.

[1] G.S. Oehrlein et al., J. Appl. Phys. **108**, 043307 (2010)
[2] M. A. Golub and T. Wydeven, Polym. Degrad. Stabil. 22, 325 (1988)
[3] E. Vietzke and V. Philipps, Fusion Technol. 15, 108 (1989)
[4] A Erradi, R. Clergereaux, and F. Gaboriau, J. Appl. Phys. 107, 093305 (2010)
[5] O. Kylián et al., Plasma Process. Polym. **5**, 26 (2008)
[6] R. C. Seid, W. M. Bone, and L. R. Phillips, Anal. Biochem. 155, 168 (1986)
[7] J. W. Jones et al., PNAS, 105, 12742 (2008)
[8] M. M. Wurfel et al., J. Immunol. 175, 2570 (2005)

Contributed Presentations at Conferences:

1. E. Bartis, J. Seog, G.S. Oehrlein, T.-Y. Chung, N. Ning, J.-W. Chu, D.B. Graves, "Deactivation of Lipopolysaccharide and Lipid A by Ar/H_2 Inductively Coupled Plasma," AVS International Symposium, Nashville 2011.
2. T.-Y. Chung, N. Ning, J.-W. Chu, D.B. Graves, E. Bartis, J. Seog, G.S. Oehrlein, "Plasma Deactivation of Pyrogenic Biomolecules: Vacuum Ultraviolet Photons and Radical Effects on Lipid A," AVS International Symposium, Nashville 2011.

Year 3 Progress Report, June 2013: Activities and Findings

Plasma Processing and Materials Characterization at UMD

Activities: Year 3 Update

In this **progress report**, we present an update on the project, including the development and characterization of an atmospheric pressure plasma jet (APPJ) and key low pressure studies that clarify the ELISA method at **UMD**. Figure 1a shows a schematic of the APPJ, which consists of two electrodes wrapped around an alumina tube that are separated by an insulator. Ar gas with up to a two percent admixture of O_2/N_2 flows through the alumina tube. When an AC high voltage is applied between the electrodes, the plasma ignites. The spacing between the two electrodes can be varied as well as the position along the tube. Varying the position along the tube changes the source-to-sample distance, *s*, and allows us to control the flux of various reactive species at the sample. At low values of *s*, charged species dominate while radical species play a larger role when this distance is increased. At longer values of *s*, only long-lived species such as ozone and NO_x can reach the sample. The jet has been characterized by optical emission spectroscopy for detection of excited species and ultraviolet absorption spectroscopy for detection of ozone. Deactivation by the APPJ was measured using ELISA and surface chemistry changes in air and a controlled environment were measured with XPS. For XPS experiments, the APPJ was mounted in a vacuum chamber, as shown in Fig. 1b. We explored two scenarios with different levels of interaction of the APPJ plume with the environment and find that this interaction is very important for studying surface modifications.

Undergraduate student Caleb Barrett continued his research experience by performing experiments with high voltages and at atmospheric pressure. Caleb also had the opportunity to train a **new undergraduate student, Connor Hart** on the various techniques we use in our laboratory, which extended Connor's physics background to biology-related fields. Connor also contributed substantially to the initial development of the APPJ.

Findings: Year 3 Update

APPJ Work. For the APPJ system studied at **UMD** we find that small changes to the feed gas chemistry significantly impact the plasma properties. Figure 2a shows the emission due to atomic O (O*) and the second positive system of N_2 (N_2*, $C\ ^3\Pi_u \rightarrow B\ ^3\Pi_g$) at 777 nm and 337 nm, respectively, relative to the Ar emission at 750 nm. The 750 nm Ar emission peak has been extensively studied and reflects the plasma density as this peak is excited by electron impact excitation from the ground state.[1] When Ar without N_2/O_2 admixtures is used, nominal levels of N_2* and O* are detected due to interactions with the ambient and trace impurities from the gas bottle; the plasma is dominated by Ar ions and metastables. Adding up to 0.66% O_2 to Ar causes a marked increase in atomic O. Adding N_2 to the discharge causes a major increase in N_2* emission that does not saturate in the range explored. At 1% N_2 addition, N_2* emission is already nearly 4 times larger than the Ar emission. This effect can also be observed by the naked eye as the discharge changes color from white to violet. For a 1:1 O_2/N_2 mixture, O* emission saturates

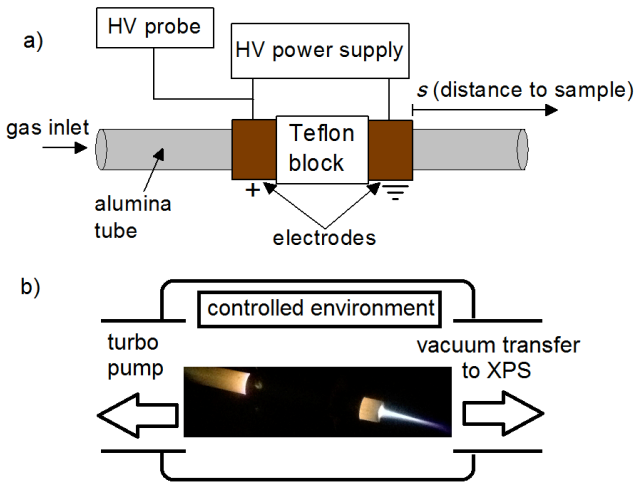

Figure 5. *(a) A schematic representation of the atmospheric pressure plasma jet (APPJ). (b) The APPJ is mounted inside a vacuum chamber where the environment can be controlled during the treatment as shown. After the treatment, the samples are vacuum transferred to XPS for surface analysis.*

at the same admixture, but N_2*emission drops to less than the Ar emission in the admixture range explored. These observations can be explained as follows: when only N_2 is added to the plasma, N_2* increases as more nitrogen is added as there are few species with which N_2* can react. However, when O_2/N_2 mixtures are used, N_2* can react with oxygen species to form NO, NO_2, N_2O, etc. Spatially-resolved optical emission spectroscopy of the APPJ operating with pure Ar (not shown due to space limitations) shows a clear increase in N_2* emission as the distance from the jet nozzle is increased due to the plasma interacting with the environment.

UV absorption was used to measure ozone produced by the APPJ. Increasing the O_2 admixture increases the ozone produced by the APPJ through the reaction:

$$O + O_2 + M \rightarrow O_3 + M \qquad (1)$$

where M is any specie that can stabilize the reaction such as Ar, O_2, or the alumina tube itself. Ozone densities as high as 10^{15} cm^{-3} were reached with O_2 admixtures less than 2%. Increasing the voltage destroys some of the ozone due to dissociation of O_3 into O_2 and O.

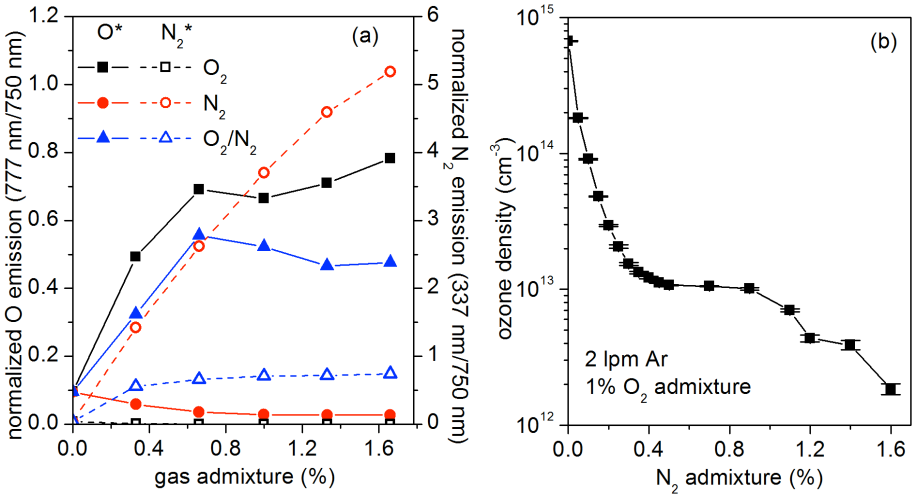

Figure 2*: (a) Emission due to atomic O and the second positive system of N_2 normalized to the Ar emission at 750 nm. (b) Ozone produce by the APPJ can be dramatically reduced by small admixtures of N_2*

to an ozone producing condition.

Figure 2b shows that adding small admixtures of N_2 to ozone producing conditions causes a dramatic decrease in the ozone density by up to nearly 3 orders of magnitude. This effect, called discharge poisoning, has been widely studied by ozone scientists and results from cyclic reactions where nitrogen species consume ozone and atomic O to form NO, NO_2, NO_3, and O_2.[2]

The effect of gas chemistry and source-to-sample distance, *s*, on biodeactivation of bLPS was examined. Figure 3(a) shows the differences between 1% N_2 in Ar, 1% and 0.2% O_2 in Ar, and 1% synthetic air (1:4 O_2/N_2) in Ar plasmas under radical-only conditions. N_2/Ar plasmas show very little deactivation due to the lack of reactive species. On the other hand, O_2/Ar plasma shows strong deactivation due to formation of reactive oxygen species. 1% air admixtures also show strong deactivation, but less than in the 1% O_2 admixture case. Note that when 0.2% O_2 is added, which has the same O_2 content as the 1% air admixture, we observe higher deactivation than the air admixture. This is due to the consumption of the more reactive oxygen species (e.g. atomic O) during the formation of NO_x. Figure 3b shows that as the source is brought closer to the sample, increased deactivation is observed due to the increased flux of reactive species reaching the sample, as expected. When the source gets very close to the sample, charged species begin to interact with the film and cause complete deactivation.

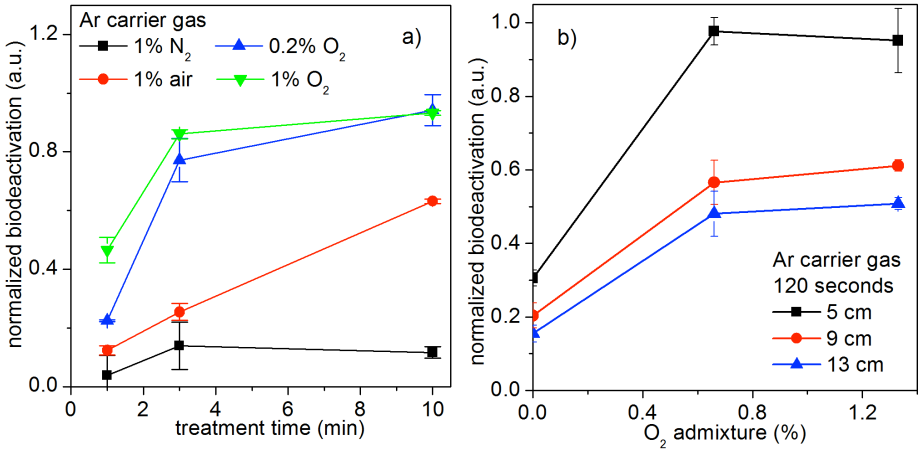

***Figure 3**: (a) Normalized biodeactivation vs. treatment time for four different gas chemistries in the confined geometry. The N_2 admixture causes minor deactivation, while O_2-based discharges show clear deactivation. For the same O_2 admixture, less deactivation is observed if N_2 is added, demonstrating the quenching effect of reactive nitrogen species with reactive oxygen species to form less reactive NO_x species. (b) As s is decreased, more reactive species reach the sample and causing increased deactivation.*

Surface analysis was performed on LPS films after APPJ treatment. Experiments were performed in controlled N_2/Ar environment and then vacuum transferred to XPS. The controlled environment and subsequent vacuum transfer to XPS is critical as only minimal changes will take place following plasma exposure. The use of a controlled environment to study surface modifications due to atmospheric pressure plasma is virtually non-existent in the literature.[3, 4] We find that the interaction of the jet with the environment is a major factor for determining which species reach the sample. Samples were treated under two conditions. In the first case, the source is 2 mm from the end of the alumina tube. With this geometry

(exposed), the plasma interacts with the environment due to the source's position at the end of the nozzle. In the second case, the source was 9 cm from the nozzle of the alumina tube. With this geometry (confined), plasma-environment interactions are minimized. In both cases, the tube nozzle was 4 cm from the sample. The results for the exposed scenario are completely consistent with the quenching of oxygen species by reactive N_2 observed by OES, ozone detection, and ELISA. Figure 4a shows spectra after treatment with the plume exposed in N_2, 60% N_2 in Ar, and 20% N_2 in Ar environments. Increased surface modifications occur as environmental N_2 is reduced. In the C 1s, C-C bonding decreases while O-C-O/N-C=O and O-C=O slightly decrease. In the N 1s, N-C/N-C=O and NR_4^+ slightly decrease while a peak at 408 eV due to N_2O or NO_3 emerges. This peak is strongest in the 20% N_2 in Ar environment. In the O 1s, oxygen content increases as environmental N_2 decreases. Figure 4(b) shows spectra in the 60% N_2 in Ar environment after treatment with the plume confined. Comparing the two geometries shows that the qualitative changes are similar, but intensified. Even though the plasma is farther away from the sample, the surface is more oxidized than in the exposed case, with a substantial decrease in C-C bonding, which is chiefly found on the aliphatic chains of lipid A.

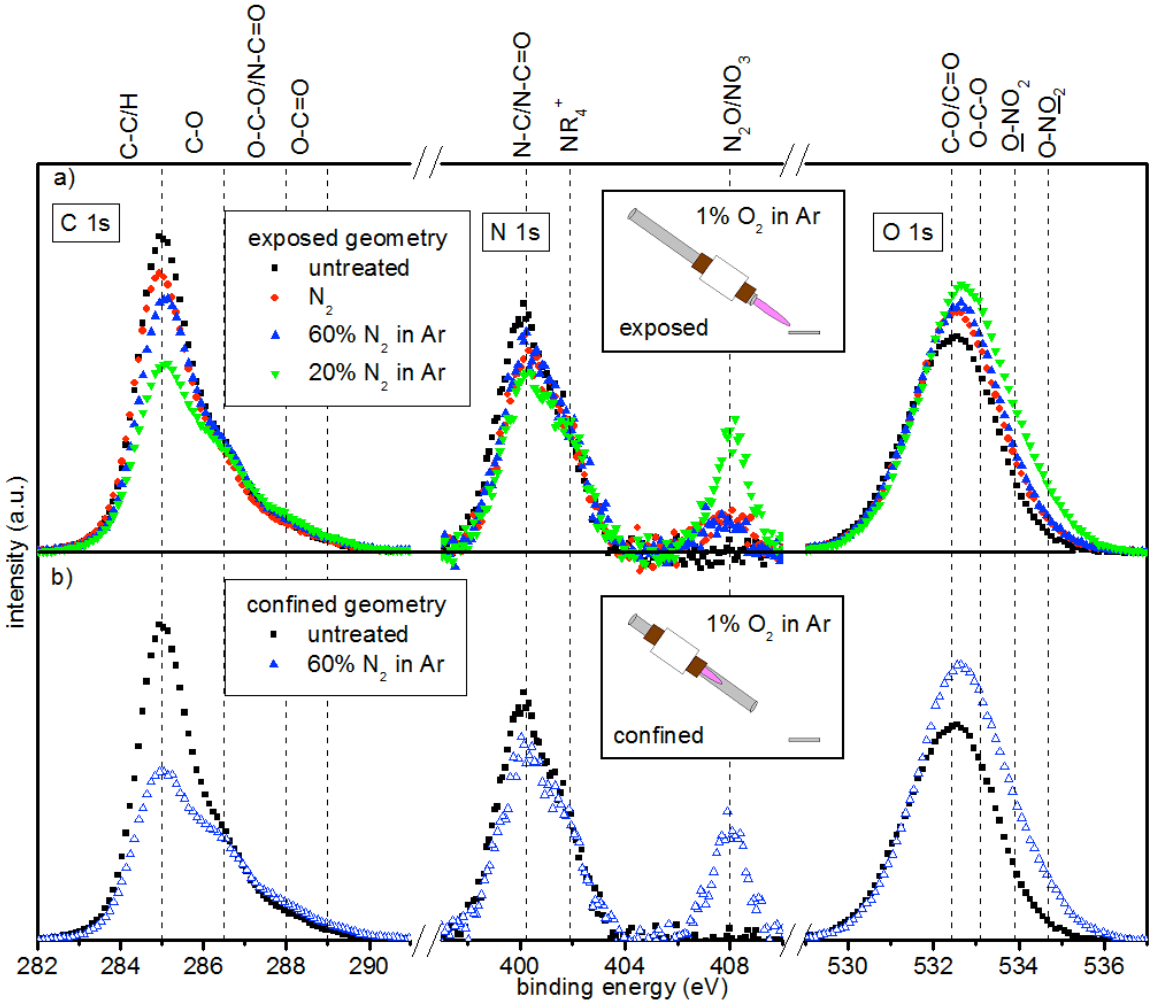

Figure 4: *XPS C 1s, N 1s, and O 1s spectra of (LPS) films after treatment in N_2/Ar environments for conditions where the plasma is (a) exposed to the environment and (b) confined within the*

alumina tube. Increasing N_2 concentrations in the environment quench reactive oxygen species that would otherwise oxidize the sample.

The loss of C-C bonding due to atomic O is consistent with work performed at **UCB** where O atoms reduced the number of intact aliphatic chains on lipid A as measured by ToF-SIMS.[5] Transferring samples to XPS through air instead of vacuum was also studied (omitted here due to space limitations) and showed that oxidation of the surface was decreased, indicating that weakly-bound surface species are removed by exposure to ambient conditions. It is clear that the interaction of the jet with the environment plays a major role with regard to which species reach the sample. As the nozzle-to-sample distance remained constant for both geometries, N_2 in the environment is not a significant quencher of ROS, which suggests that the excitation of N_2 species is required.

Low Pressure Plasma Work Performed at UMD. Previous ELISA experiments had been conducted with a microtiter plate using a low bLPS concentration of 100 ng/ml. We furthered our ELISA studies by studying the effect of increasing this concentration to as high as 50 ug/ml. After low pressure Ar treatment, we find that higher concentrations deposited in the well, which correspond to more material in the well, show less deactivation. This finding suggests that, for Ar plasma, etching is required for deactivation, rather than just surface modifications. In contrast, H_2 plasma treatment under the same conditions causes faster deactivation, suggesting that radical-induced surface modifications, in addition to etching, are important for H_2 plasma. The radical effect is also seen as deactivation is higher after H_2 treatment for similar levels of material removal, as shown in figure 5. We hypothesize that lower concentrations show increased deactivation due to reduced LPS thickness (in the extreme incomplete coverage of the well) which allows for increased plasma-material interactions due to relatively more exposed and plasma modified LPS material for the low bLPS concentration studies. By XPS, we observed that H_2 plasma treatment reduces the oxygen content of LPS films. The removal of oxygen reduces key functional groups such as carbonyls, which are likely required for biological activity.

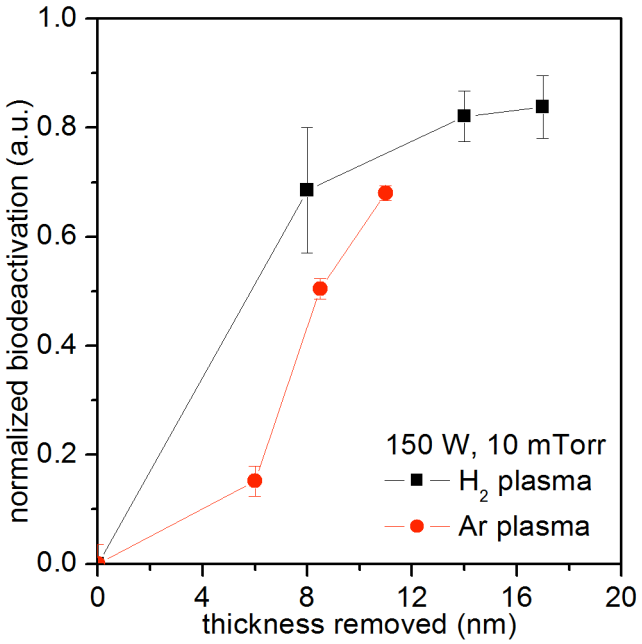

***Figure 5**: normalized biodeactivation as a function of thickness removed for direct Ar and H_2 plasma treatments. H_2 plasma treatment shows enhanced deactivation for similar levels of material removal due to radical-induced surface modifications.*

At **UMD**, our next steps include further characterization of the atmospheric pressure plasma jet by spatially-resolved optical emission spectroscopy, UV absorption spectroscopy, laser induced fluorescence and two photon absorption laser induced fluorescence, as well as high speed photography. We also will conduct further surface analysis of films in controlled environments under various plasma conditions. The obtained results will be compared to atmospheric pressure sources studied at **UCB**.

Plasma Processing and Materials Characterization at UC Berkeley

Activities: Year 3 Update

In this **progress report**, we present an update on the project at **UC Berkeley**. The first topic presented is: Lipid A deactivation by indirect air dielectric barrier discharge and UV/ozone cleaner.

An atmospheric pressure, indirect air dielectric barrier discharge (DBD), also called surface micro-discharge (SMD), has been used in the Graves lab to study gas phase and liquid phase (when present) chemistry and in some cases, the resulting surface and aqueous antimicrobial effects. It was found that when the input power was lower than ~ 0.1W·cm^{-2}, the gas phase ozone density increased monotonically with power to a concentration over 1000 ppm in a confined volume. Besides ozone, the presence of various other species, including N_2O and N_2O_5, were also predicted by simulation and characterized by transmission Fourier

transform infrared (FTIR) spectroscopy. In contrast, when the input power was higher than ~ 0.1W·cm^{-2}, the ozone density started to decrease after a few tens of seconds. This was provisionally attributed to ozone quenching reactions with nitrogen oxides that were created by vibrationally excited nitrogen molecules reacting with O atoms at a higher power density. Under these conditions, the density of NO_2 increased as well as HNO_3. In other words, the low-power mode is ozone-rich and the high-power mode is NO_x rich.

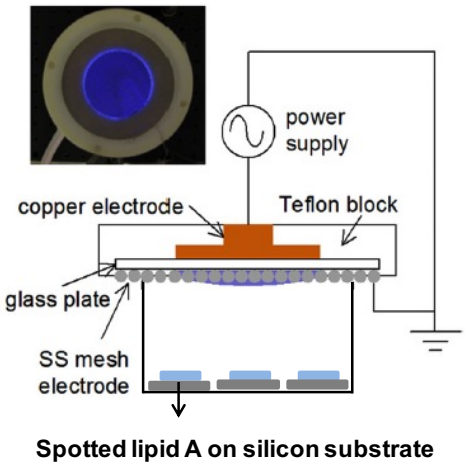

***Figure 6**: The schematic of the indirect air DBD device.*

Preliminary experiments were carried out to study lipid A deactivation by indirect air DBD in a confined reactor. The schematic of the system setup is shown in Figure 6. The distance between samples and the stainless steel mesh was about 40 mm. Two sets of DBD conditions were chosen: low-power mode (0.05W·cm^{-2}) and high-power mode (0.25W·cm^{-2}). Samples were also processed with a commercial UV-ozone cleaning system (UVOCS®, Lansdale, PA, USA) operated under ambient condition. The ozone was generated by a low-pressure quartz mercury vapor lamp in the UV-ozone cleaner. Processed samples (10 µl, 0.2 mg·ml^{-1}) were then characterized by ex situ FTIR and human whole blood tests.

Figure 7 shows the FTIR spectra (CH_2/CH_3 region) of samples processed with DBD in both low-power mode and high-power mode along with samples treated by the UV ozone cleaner. While both DBD modes result in minimal change of processed samples, the UV ozone cleaner shows high level of mass removal.

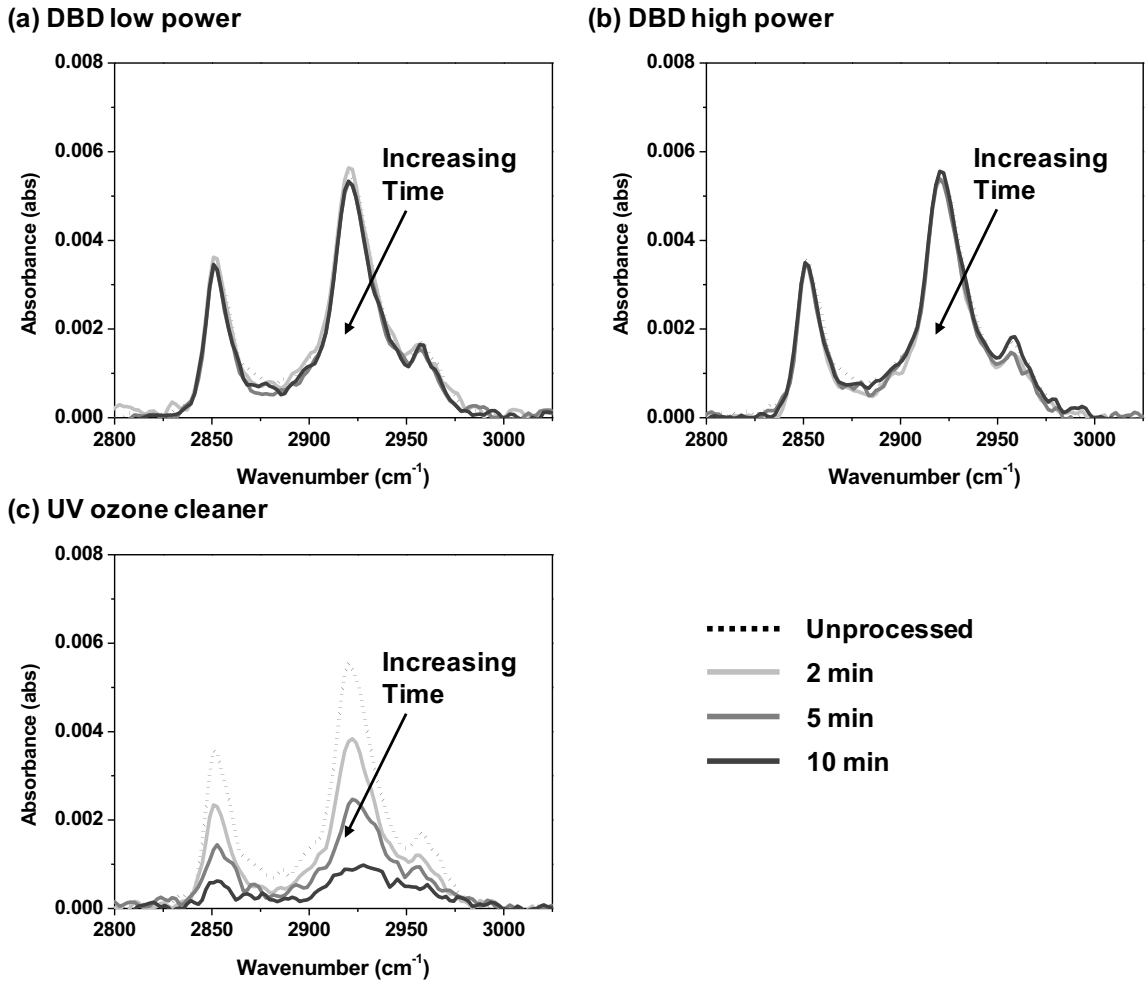

***Figure 7**: Transmission FTIR spectra of lipid A CH_2/CH_3 region (2800–3025cm^{-1}) after various exposures: (a) DBD low power, (b) DBD high power (c) UV ozone cleaner. Each condition is an average of three independent measurements.*

Figure 8 shows the endotoxic activity of processed lipid A samples, which was monitored by measuring the secreted IL-1β in human whole blood from 1 healthy donor. For most conditions, the suppression of IL-1β is not observed. The results obtained from samples processed with the UV ozone cleaner are especially surprising. The IL-1β secretion change with different exposure times does not correlate with the observed dramatic mass reductions observed with FTIR in Figure 7.

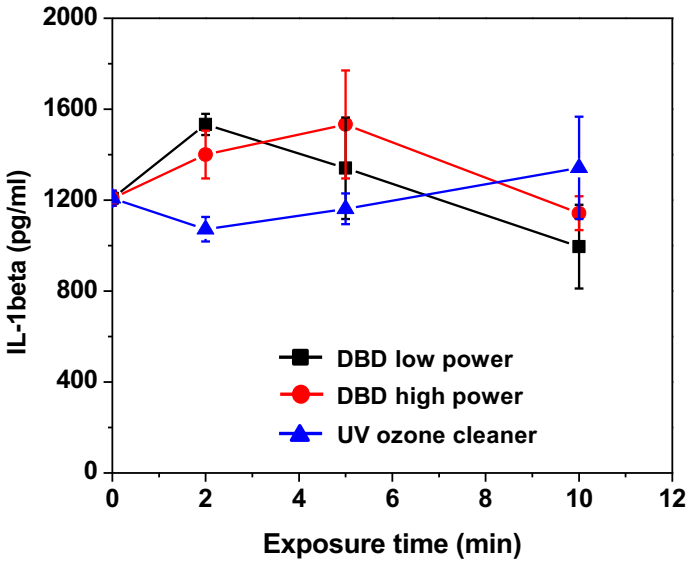

Figure 8: *Endotoxic activity monitored by secreted IL-1β in human whole blood assay. Measurements were conducted with blood from 1 healthy donor. The error bar for each data point stands for the standard deviation from 3 independent exposure samples.*

We note that the experimental conditions here (e.g.: the operation pressure, the reactive species involved, the flux of reactive species) are very different from the low pressure studies reported previously. While these preliminary results suggest that indirect DBD may not be a promising option for surface deactivation of lipid A, the UV ozone-cleaner results are surprising and counter-intuitive. The low-pressure plasma/beam results suggest that removal and alteration of lipid A will generally reduce the immune response. But the UV-ozone exposure removes a significant fraction of the film without altering the apparent endotoxic activity of the remaining film. Tthe immune response is complex and not fully understood. It consists of various coupled, intertwined pathways. One possibility is that simple mass removal of lipid A may not be sufficient to reduce endotoxicty because the remaining residues or byproducts activate other pathways, and thus the overall inflammation response is not mitigated. This also highlights the challenge of deactivating virulent biomolecules in a clinical setting. Further studies on molecular/cellular level mechanisms are required in order to further pursuit atmospheric pressure plasma application on biological targets.

The second topic presented is: **Anti-inflammatory effects of indirect air dielectric barrier discharge-treated water.**

Published studies have shown that oxidized low-density lipoprotein (OxLDL) and 'ozonized' amino acids present anti-inflammatory effects that suppress generation of cytokines from cells. It is known that upon stimulation by tumor necrosis factor (TNF), cells pre-incubated with ozonized medium showed a suppressed activation of transcription factor NF-κB and secretion of Interleukin-1β (IL-1β). Ozonized amino acids, such as cysteine and tryptophan, are important components responsible for the anti-inflammatory effects.

When operated at low power (~ 0.1W·cm^{-2}), indirect air dielectric barrier discharge (DBD) can be used to generate mainly ozone. Aqueous solutions treated by DBD (cf. Fig 6) operated at low power can result in high concentration of aqueous ozone. It was suspected that DBD-treated water might lead to a similar anti-inflammatory effect.

Figure 9 shows the schematic of the setup. 5 ml of phosphate-buffered saline solution (PBS, catalog number: 10010, Life Technologies, Grand Island, NY, USA) or RPMI medium 1640 (catalog number: 21870, Life Technologies) was placed in a small petri dish and treated with DBD for 10 min. The solution was mixed with fresh human whole blood shortly after generation. The DBD operation power was fixed at 0.05 W·cm^{-2}. The gap between the liquid surface and the stainless steel mesh was about 5 mm. The protocol of human whole blood test is shown in Figure 9. 500 µl of fresh human whole blood was pre-incubated with 500 µl DBD-treated solution for 45 min. 5 µl of lipopolysaccharide (LPS) solution (1µg·ml^{-1}) was then used to stimulate leukocytes in whole blood. After another 22-hour incubation, the supernatants were collected after centrifugation for 10 minutes at 400×g and stored at -20˚C until IL-1β contents were determined by a commercial enzyme-linked immunosorbent assay (ELISA) from Life Technologies.

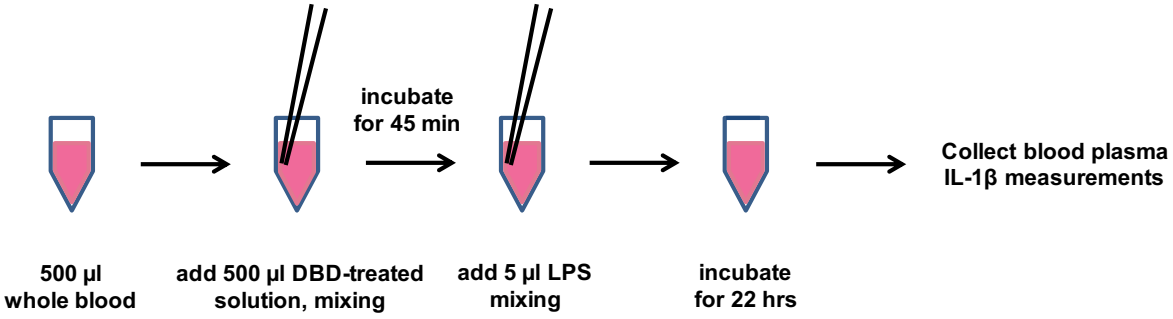

Figure 9: *Protocol of air DBD-treated solution tests.*

Sample condition	Liquid Medium	DBD-treated water (500 µl)	LPS (5 µl, 1µg·ml^{-1})
1	PBS	-	-

2	PBS	-	+
3	PBS	+	-
4	PBS	+	+
5	RPMI	-	-
6	RPMI	-	+
7	RPMI	+	-
8	RPMI	+	+

Table 1. *Experimental conditions used in this study. Four samples were prepared for each condition. Three were for human whole blood tests and one was for cell viability determination by trypan blue exclusion.*

Experimental conditions are tabulated in Table 1. Figure 9 shows the IL-1β expression resulted from various treatments. Blood cell viability was monitored by trypan blue exclusion with a hemacytometer. No obvious cell death was observed after incubation.

Pristine PBS and RPMI without LPS do not stimulate IL-1β secretion. Without stimuli LPS, DBD-treated PBS and RPMI also show minimal inflammatory effects. On the other hand, the presence of LPS induces IL-1β expression, probably through the Toll-like receptor 4 (TLR-4) pathway. For blood pre-incubated with DBD-treated PBS, the IL-1β concentration is suppressed to about 75% of that pre-incubated with non-DBD-treated PBS. The result can be attributed to aqueous ozone oxidizing amino acids in blood serum. These modified amino acid molecules then interact with cellular signaling pathway and inhibit secretion of IL-1β. On the other hand, DBD-treated RPMI shows no clear anti-inflammatory effect. We observed that the color of RPMI faded after DBD treatment. It is suspected that aqueous ozone is consumed by reacting with phenol red (pH indicator in RPMI) and thus DBD-treated RPMI has no effect in IL-1β generation. Future experiments should pursue using RPMI without phenol red to verify this speculation.

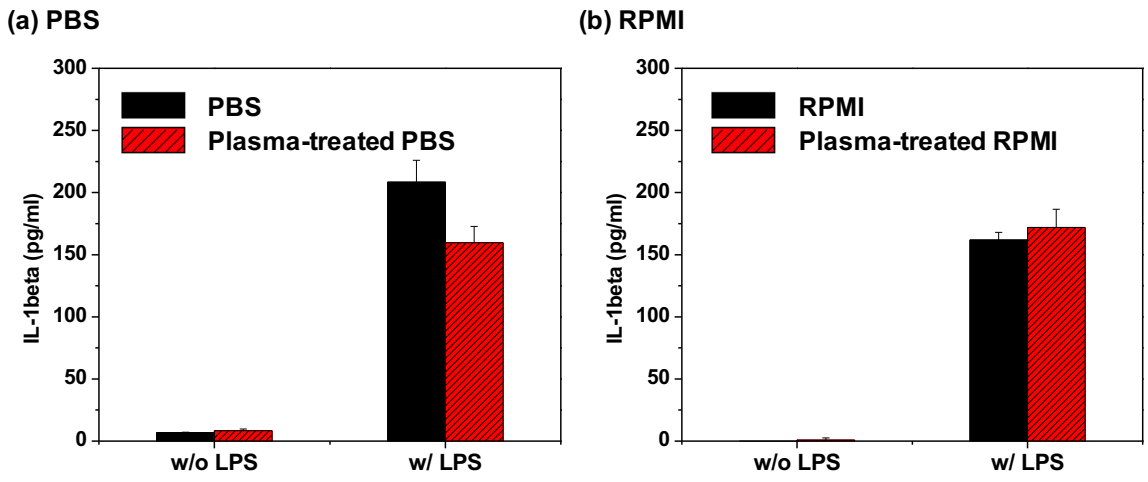

Figure 10: *Endotoxic activity monitored by secreted IL-1β in human whole blood assay. The liquid media were (a) PBS and (b) RPMI. Measurements were conducted with blood from 1 healthy donor. The error bar for each condition stands for the standard deviation from 3 independent samples.*

While disinfection effects of plasma or DBD-treated solutions have been demonstrated previously, the possible therapeutic effects of discharge-activated water suggests a new direction for exciting applications. However, these results are preliminary and require further studies. New assays have to be applied to identify the detailed inhibition mechanism and anti-inflammatory products generated by aqueous ozone or other discharge-generated species.

Contributed Presentations at Conferences:

1. E. Bartis, J. Seog, G.S. Oehrlein, T.-Y. Chung, N. Ning, J.-W. Chu, D.B. Graves, "Deactivation of Lipopolysaccharide and Lipid A by Radicals Produced in Inductively Coupled Plasmas," AVS International Symposium, Tampa 2012.
2. T.-Y. Chung, N. Ning, J.-W. Chu, D.B. Graves, E. Bartis, J. Seog, G.S. Oehrlein, "Low Temperature Plasma Deactivation of Endotoxic Biomolecules: the Effects on Lipid A," AVS International Symposium, Tampa 2012.
3. E. Bartis, C. Hart, H.-W. Chang, D.B. Graves, J. Seog, G.S. Oehrlein, "Deactivation of Lipopolysaccharide by an Atmospheric Pressure Plasma Jet," DOE Plasma Science Center 4th Annual Meeting, College Park 2013.

Publications:

1. T.-Y. Chung, N. Ning, J.-W. Chu, D.B. Graves, E. Bartis, J. Seog and G.S. Oehrlein, "Plasma Deactivation of Endotoxic Biomolecules: Vacuum Ultraviolet Photon and Radical Beam Effects on Lipid A", Plasma Processes and Polymers **10** (2), 167-180 (2013).
2. E.A.J. Bartis, D.B Graves, J. Seog, and G.S. Oehrlein, "Atmospheric pressure plasma treatment of lipopolysaccharide in a controlled environment", Journal of Physics D: Applied Physics, Fast Track Communication (submitted, 2013)
3. E.A.J. Bartis, J. Seog, G.S. Oehrlein, T.-Y. Chung, J.-W. Chu, and D.B Graves, "Characterization of Atmospheric Pressure Plasma Jet Fed with $Ar/O_2/N_2$ for Deactivation of Lipopolysaccharide", Plasma Processes and Polymers (in preparation, 2013).
4. E.A.J. Bartis, J. Seog, G.S. Oehrlein, T.-Y. Chung, J.-W. Chu, and D.B Graves, "Deactivation of Lipopolysaccharide and Lipid A by Ar/H_2 Inductively Coupled Low Pressure Plasma", Plasma Processes and Polymers (to be submitted, 2013).

References:

1. J. P. Booth, O. Joubert, J. Pelletier and N. Sadeghi, Journal of Applied Physics **69** (2), 618-626 (1991).
2. U. Kogelschatz, Plasma Chemistry and Plasma Processing **23** (1), 1-46 (2003).
3. E. Gonzalez, II and R. F. Hicks, Langmuir **26** (5), 3710-3719 (2010).
4. J. Xu, C. Zhang, T. Shao, Z. Fang and P. Yan, Journal of Electrostatics **71** (3), 435-439 (2013).
5. T.-Y. Chung, N. Ning, J.-W. Chu, D. B. Graves, E. Bartis, S. Joonil and G. S. Oehrlein, Plasma Processes and Polymers **10** (2), 167-180 (2013).

Year 4 Final Progress Report, Sept. 2014: Activities and Findings

Plasma Processing and Materials Characterization at UMD

Activities: Year 4 Update

In this **final report**, we present a final update on the project. During the final year of this grant we continued the characterization of the effluent of an atmospheric pressure plasma jet (APPJ) and plasma-induced modifications of polymer surfaces at **UMD**. We continued our work in controlled environments, where we compared O_2 and N_2 ambients for the confined and exposed geometries for $O_2/N_2/Ar$ plasmas. We chose to study model polymers to simplify the complex molecular structure of typical bio-molecules studied in this project, e.g. LPS. This approach allows to distinguish surface-bound oxygen and nitrogen species originating from the polymer from those formed in the gas phase. We chose to study films composed of only carbon or only carbon and oxygen including polystyrene, poly(methyl methacrylate), 193 nm photoresist, and 248 nm photoresist. To further characterize how the environment impacts the plasma, we used high speed photography to compare how the plume changes when the ambient is changed from air to one that matches the feed gas. High speed photography was also used to observe plasma-surface interactions when the plume is electrically-coupled to the surface. We additionally developed a UV absorption measurement system to more accurately measure O_3 densities.

Undergraduate student Connor Hart continued his research experience by setting up and conducting experiments to characterize the effluent of the APPJ. This extended his previous research, which focused more on biological deactivation and surface analysis, to spectroscopy and modelling. **A new undergraduate student, Brian Crump,** was brought onto the project. His efforts expanded his mechanical engineering background into surface analysis and vacuum science.

Findings: Year 4 Update

After APPJ treatment using Ar, Ar/N_2 or Ar/O_2 gases, we find that each of the polymers was oxidized by APPJ treatments with new chemical moieties created during the interaction, e.g. C-O, O-C-O/C=O, O-C=O, and even highly oxidized species such as O-(C=O)-O. By varying APPJ treatment parameters such as treatment time, feed gas chemistry, source geometry, and ambient gas chemistry, we were able to form these moieties in different ratios. In our previous reports, we observed the formation of a new chemical species on LPS surfaces that we attributed to NO_3. We find that this species forms on each of these polymers as well despite the major differences in chemical structure among the biomolecule and polymers. This species has been modelled as a key species in the far effluent of APPJs [i], but, to the best of our knowledge, it has not yet been measured on APP-treated surfaces. Continuing our investigation

with studies in well-controlled environments, we specifically focused on polystyrene as it contains only hydro-carbon bonds [ii].We compared how O_2 and N_2 controlled environments impact polystyrene surface modifications for O_2, N_2, and Air admixtures to an Ar APPJ in confined and exposed geometries. One key result was that, even though O_2 admixture to the feed gas greatly enhances surface oxidation and biodeactivation, the O_2 ambient lead to reduced surface modifications compared to the N_2 ambient. Figure 1 shows high resolution XPS spectra of polystyrene films treated by 1% O_2/Ar plasma in the confined geometry in O_2, air, and N_2 environments. As environmental O_2 is reduced, surface modifications both in the form of overall oxygen uptake and NO_3 formation increase. Ambient O_2 will readily react with radicals in the polymer to form a peroxy radical, which can form alcohol and carbonyl groups. In the N_2 ambient, this cannot occur as quickly, leaving the surface radical sites open to attack by plasma-generated ROS. This finding demonstrates the possibility to regulate the flux and type of reactive species reaching a target surface by controlling the environment between the plasma source and surface.

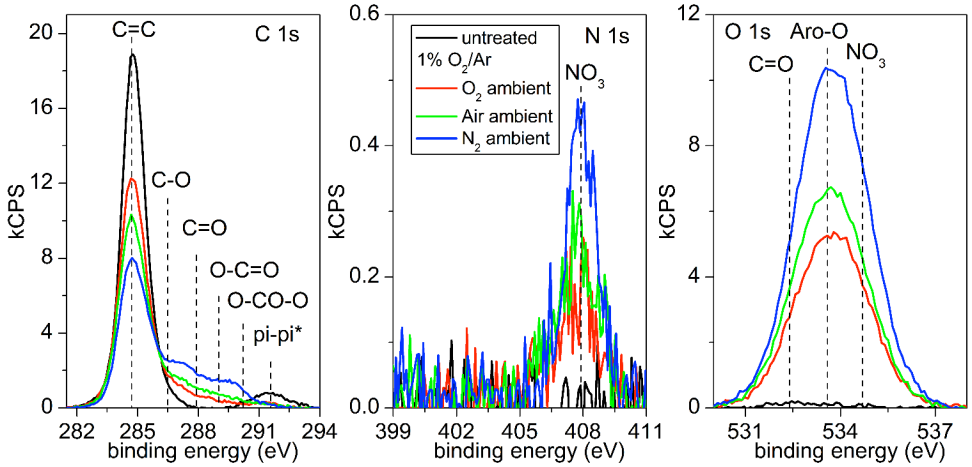

Figure 1: High-resolution XPS spectra of polystyrene treated by O_2/Ar APP in O_2, Air, and N_2 environments in the confined geometry.

The feed gas chemistry also affects the surface modifications, which is consistent with the previously reported major impact on biological deactivation of LPS, optical emission, and O_3 density. Ar plasma causes the most modifications when exposed to the ambient in O_2 due to excitation and dissociation of ambient O_2 by electrons and metastables. In the N_2 ambient, the O_2-deficient conditions cause minimal modifications. N_2/Ar feed gas did not effectively deactivate LPS films, and we find that surface modifications are minimal, but strongest when the plasma is exposed to O_2. Even though the Air/Ar plasma has O_2 in the feed gas, the N_2 content is so high that less reactive species such as N_2O form.

A study of a variety of feed gases in both geometries and environments established a possible correlation between oxygen composition and nitrogen composition in treated films. We distinguished three modes of modification that depend on the availability of O_2, as shown in figure 2. For O_2/Ar APPJ treatment, enough ROS are generated in the source to lead to strong surface oxidation regardless of the geometry or environment, which only impact the oxidation rate. Little nitrogen incorporation is seen under these conditions. For Ar, N_2/Ar, and Air/Ar APPJ

treatments, two additional regimes exist depending on the ambient chemistry. For the O_2 ambient, NO_x species become more relevant, but oxidation is still rapid since ambient O_2 can interact with plasma-generated species as well as radical sites on the surface to form peroxy radicals and hydroperoxide groups, which are known to result in a variety of oxygenated species [iii]. For the oxygen-deficient treatment conditions in the N_2 ambient, modifications more strongly depend on NO_x species to activate the surface. We note here that, even though Air/Ar treatment has O_2 in the feed gas, the N_2:O_2 ratio is so high that less reactive species such as N_2O and N_2O_3 are formed instead of more reactive NO_3 species. In fact, for the N_2/Ar feed gas exposed in the N_2 environment, we measure NO and NO_2 on the surface in addition to NO_3. However, if the oxygen composition is plotted against only NO_3 instead of the sum of all NO_x species for this condition, then the trend follows that of the O_2/Ar treatment (see Fig. 2a, exposed NO_3-only). This indicates that NO_x is a key species required for oxidation and that if ROS are not produced directly in the discharge as in the O_2/Ar plasma, then surface oxidation proceeds via formation of NO_3 at the surface. The reactive uptake of various gas phase RONS including NO_2, NO_3, HNO_3, N_2O_5, and O_3 by polycyclic aromatic hydrocarbon (PAH) surfaces has been studied by Gross et al. [iv]. They report that reactive uptake by NO_3 was very fast for the three PAHs studied and very slow for the other species, which agrees with our analysis.

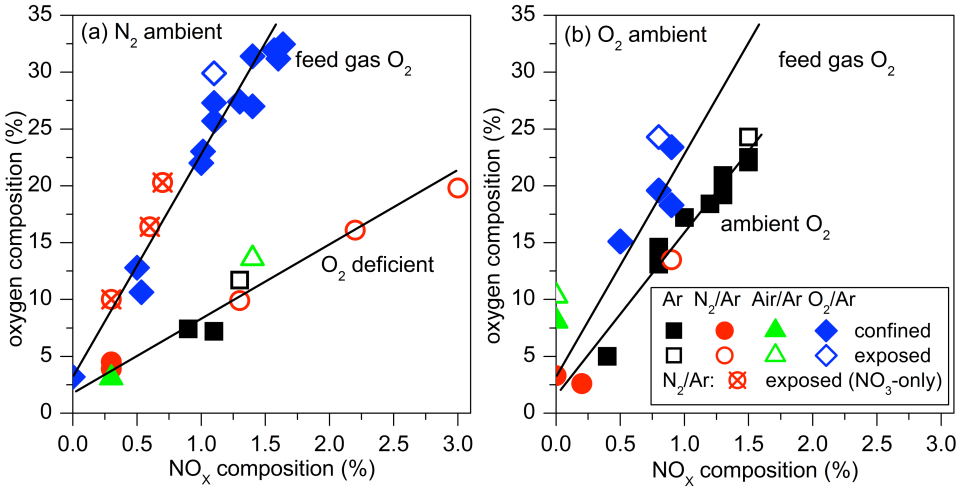

Figure 2: Oxygen composition of polystyrene films as a function of NO_x uptake for various treatment conditions.

As O_3 is a long-lived species and a strong oxidizer, the O_3 density was measured for the APPJ for applied voltages ranging from 12 kV to 18 kV as shown in figure 3. Consistent with the literature, increasing the applied voltage leads to decreased O_3 production with 12 kV producing ~6.7×10^{14} cm^{-3} over the 7 minute experiment and 18 kV producing less than 10^{13} cm^{-3} after the first ~60s due to thermal decomposition of O_3 and reduced formation at higher temperatures [v]. Even though the 18 kV treatment produces significantly less O_3, the surface modifications are actually higher with O/C ratios of 0.42 ± 0.06 and 0.37 ± 0.02 for 18 kV and 12 kV, respectively, indicating that O_3 is not a key player in surface oxidation. Studies on photodegradation of polymers have concluded that O_2* in the presence of sunlight is a potent oxidant, pointing towards the importance of this metastable species [iii]. With OES, we have measured emission down to 240 nm due to NO. Other groups have measured Ar_2*, which emits in the 115-135 nm range, in their plasma [vi]. It is well known that O_2 absorbs high energy

photons in the upper atmosphere, contributing to the O_3 layer. One key reason the O_2 ambient is less effective than the N_2 ambient for O_2/Ar APP could be due to the UV/VUV emission from the plasma being absorbed in the former and passing through the latter environment. High energy photons are known to abstract hydrogen from polymers, leadings to radical sites on the polymer [iii]. This extra pathway for hydrogen abstraction is likely responsible for the increased modifications in N_2 ambient.

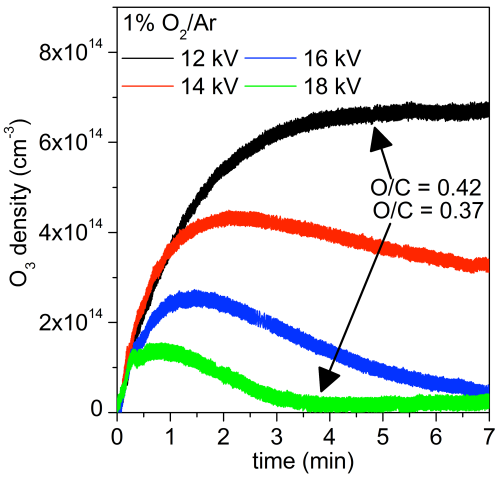

Figure 3: O_3 density over time for applied voltages between 12 kV and 18 kV.

Undergraduate student Connor Hart continued his work in the lab and worked closed with a new graduate student, Andrew Knoll. Using high-speed photography, we characterized how the APPJ effluent changes with gas chemistry and when the environment is changed from ambient air (see Fig. 3, top row) to one that matches the feed gas (see Fig. 3, bottom row) [vii]. The pure Ar plasma is confined within a narrow plume that extends in length when exposed to the Ar ambient. N_2/Ar plasma creates a wider, branched plume which becomes even more diffuse and branched when the ambient matches the feed gas. The O_2/Ar plasma behaved very differently; regardless of the environment, the plume decreases in length significantly and hardly extends past the nozzle. This behavior results from the electronegative nature of O_2. High-speed photography was also used to characterize the closely-coupled interaction between the APPJ and 193 nm photoresist surface where plasma filaments directly strike the surface. This mode of operation led to an annular etch region when the source was close to the sample and visible damaged spots on the film. While not all strikes create a spot, high strike densities positively correlate with spots, indicating that the plasma will more likely electrically couple to previously damaged spots.

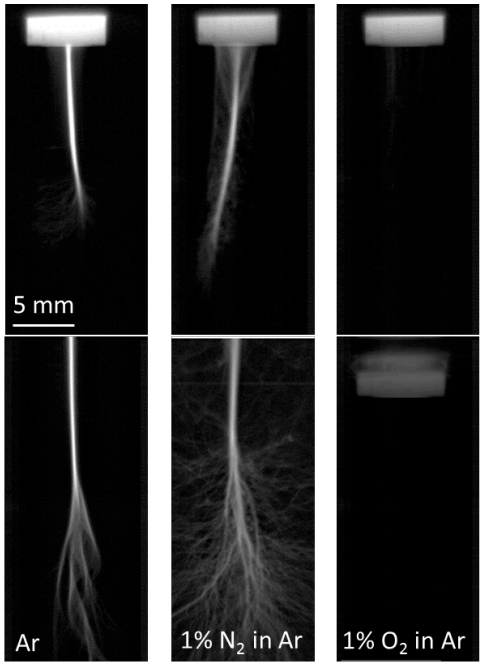

Figure 4: High speed photography in open air (top row) and enclosed environment matching feed gas chemistry (bottom row).

Plasma Processing and Materials Characterization at UC Berkeley

Activities: Year 4 Update

In this **final report**, we present a final update on the project at **UC Berkeley**. During the final year of this grant, we focused on the effect of gas flux on endotoxin lipid A deactivation at **UCB**. In particular, we used three separate types of O atom exposures of lipid A films to test the role of the magnitude of the flux on the endotoxin deactivation. This is in contrast with the earlier work we conducted that showed that endotoxin deactivation could be effected with beams of radicals in high vacuum. The results of this study have profound implications for the role and mechanisms of plasma in deactivating endotoxin films, although full interpretation must await further research.

Visiting graduate student Hungwen Chang played a key role in this research. In addition, the research was aided by collaborating scientists from the Lawrence Berkeley National Laboratory (Drs. M. Ahmed, S. Liu, and Y. Fabg); and the National Taiwan University (Prof. C.C. Hsu).

Findings: Year 4 Update

To study the effect of the flux magnitude of reactive species, a modified low-pressure inductively coupled plasma (ICP) with O radical flux ~10^{16} cm^{-2} s^{-1} was used. After ICP exposures, it was observed that while the Fourier transform infrared absorbance of fatty chains responsible for the toxicity drops by 80% through the film, no obvious film endotoxin deactivation is seen. This is in contrast to that previously observed under low flux exposure conducted in a vacuum beam system: near-surface only loss of fatty chains led to significant film deactivation. Secondary ion mass spectrometry characterization of changes at the film

surface did not appear to correlate with the degree of deactivation. Lipid A films need to be nearly completely removed in order to detect significant deactivation under high flux conditions. Additional high reactive species flux experiments were conducted using an atmospheric pressure helium plasma jet and a UV/ozone device. Exposure of lipid A films to reactive species with these devices showed similar deactivation behaviour. The causes for the difference between low and high flux exposures may be due to the nature of near-surface structural modifications as a function of the rate of film removal.

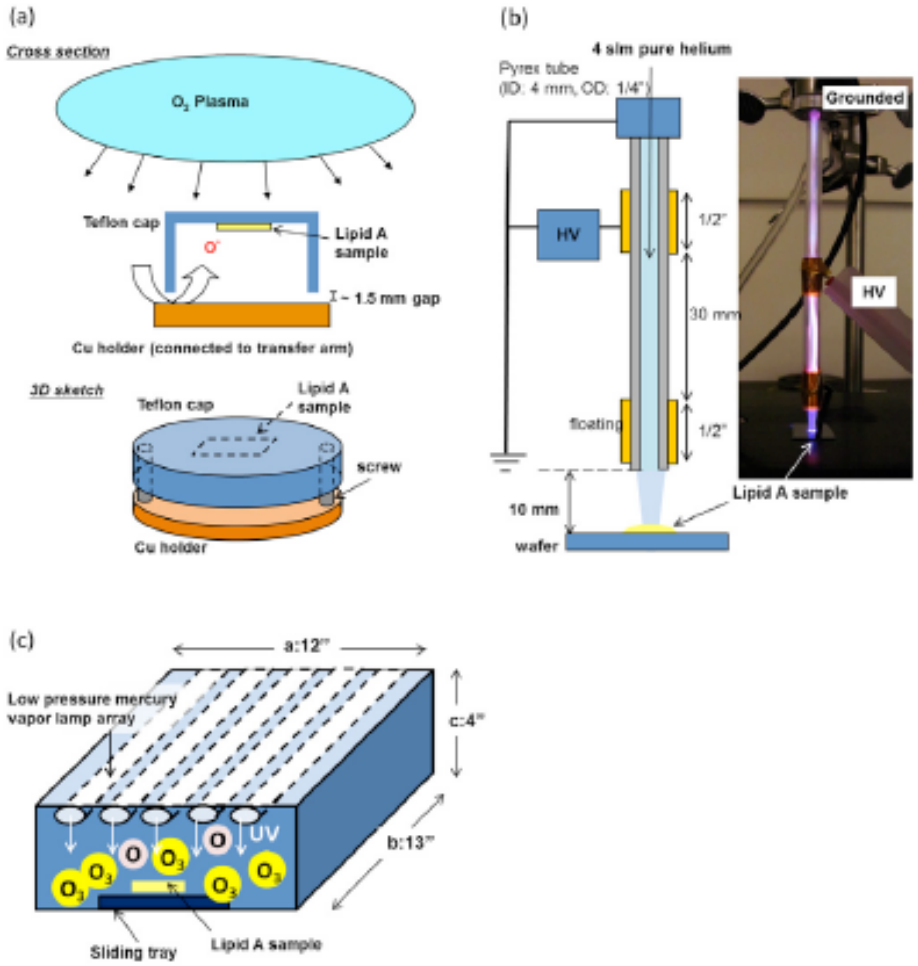

Figure 5. (a) Cross section and 3D-sketch schematic of the ICP system (b) schematic and photograph of HPJ, (c) schematic of UV/ozone cleaner.

In this study, an unexpected reactive species flux dependence of lipid A deactivation on reactive species flux is reported. In the first part of our study, the deactivation behaviour under relatively high O-radical flux exposure (1016 cm−2 s−1) in an inductively coupled plasma (ICP) is compared with a much lower radical flux (1013 cm−2 s−1) exposure in a vacuum beam system. Transmission FTIR spectroscopy measurements showed that the removal rate of the lipid A fatty acid chains is, as expected, higher under high flux exposure. However, this higher removal rate compared to the low flux beam system did not correspond to a higher rate of deactivation, contrary to expectations. After ~4 min of exposure (corresponding to an 80% drop in CH2

absorbance and therefore film loss) only about 40% reduction of IL-1β concentration was observed. 10 min of exposure was needed in order to achieve 80% endotoxin activity reduction. By plotting bioactivity (i.e. normalized IL-1β concentration) as a function of the abundance of fatty chains (normalized CH2 absorbance), two different trends are seen: bioactivity is reduced linearly and fairly rapidly with exposure under low flux, but an apparent two-phase dynamics deactivation is seen under high flux. For fractional CH2 absorbance from 1 to ~0.2, the normalized IL-1β drops from unity to ~0.6 ± 0.2 on average. When normalized CH2 absorbance drops to less than 0.2, the released IL-1β concentration drops proportionally with remaining film thickness.

In the second part of this study, an atmospheric pressure HPJ and a commercial UV/ozone cleaner were used to deactivate lipid A films. These devices also generate relatively high fluxes of reactive species and remove the films at about the same rate as the ICP system. Following the trends observed under ICP exposure, two-phase deactivation dynamics can be seen in both of these cases as well. Surprisingly, however, the SIMS surface characterization shows that the surface properties after HPJ and UV/ozone exposure are quite different from each other and from that observed after ICP exposure.

This study shows that lipid A film deactivation is sensitive to the magnitude of reactive species flux. The extent of surface modification appears to be significantly different under low and high flux conditions. The elimination of immune response correlates to the amount of immune stimuli that actually contact the leukocyte cells. In order to completely deactivate the bioactivity of lipid A, a near-complete removal or modification is apparently needed when the film is being removed at higher rates.

The importance of subtle differences in the surface and near-surface modifications introduced by different oxygen atom sources leading to large differences in measured biological deactivation is consistent with the work of Bartis et al [5]. For Ar or H2 plasma, they studied the effects of direct plasma, plasma-generated high-energy photons in the ultraviolet and vacuum ultraviolet (UV/VUV), or radicals on biological activity of lipopolysaccharide (LPS) measured using an enzyme-linked immunosorbent assay. Dependent on exposure conditions and surface modifications, they observed significant differences in the relationship of biological deactivation to the thinning of LPS. For instance, for exposure of LPS to radicals from a H2 plasma using an approach similar to that used in the present work, significant deactivation of LPS was measured for conditions where simultaneous LPS thickness loss was negligible. On the other hand, for Ar plasma exposure, significant thinning of the LPS was required before comparable changes in deactivation were measured.

Contributed Presentations at Conferences (during year 4):

1. E.A.J. Bartis, C. Hart, J. Seog, G.S. Oehrlein, H.-W. Chang, D.B. Graves, D. Burnette, I.V. Adamovich, W.R. Lempert, "Deactivation of Lipopolysaccharide by an Atmospheric Pressure Plasma Jet," AVS International Symposium, Long Beach 2013.
2. E.A.J. Bartis, A. Knoll, P. Luan, C. Hart, D.B. Graves, I.V. Adamovich, W.R. Lempert J. Seog, G.S. Oehrlein, "The Impact of Ambient Gas Chemistry on Lipopolysaccharide Deactivation and Polymer Modification by Plasma-Generated Radicals at Atmospheric Pressure," DOE Plasma Science Center 5th Annual Meeting, College Park 2014.

Publications (during year 4):

1. E.A.J. Bartis, D.B Graves, J. Seog and G.S. Oehrlein, "Atmospheric pressure plasma treatment of lipopolysaccharide in a controlled environment", Journal of Physics D: Applied Physics **46** (2013) 312002.
2. E.A.J. Bartis, C. Barrett, T.-Y. Chung, N. Ning, J.-W. Chu, D.B Graves, J. Seog and G.S. Oehrlein, "Deactivation of Lipopolysaccharide and Lipid A by Ar and H_2 Inductively Coupled Low-Pressure Plasma", Journal of Physics D: Applied Physics **47** (2014) 045202.
3. H.-W. Chang, C.-C. Hsu, M. Ahmed, S. Y. Liu, Y. Fang, J. Seog, G.S. Oehrlein and D.B. Graves, "Plasma flux-dependent lipid A deactivation", Journal of Physics D: Applied Physics **47** (2014) 224015.
4. A.J. Knoll, P. Luan, E.A.J. Bartis, C. Hart, Y. Raitses and G.S. Oehrlein, "Real time characterization of polymer surface modification by an atmospheric pressure plasma jet", Applied Physics Letters (submitted, 2014).
5. E.A.J. Bartis, A.J. Knoll, P. Luan, C. Hart, D.B. Graves, J. Seog and G.S. Oehrlein, "The Impact of Ambient Gas Chemistry on Polystyrene Surface Modification by Atmospheric Pressure Plasma", Journal of Physics D: Applied Physics (to be submitted, 2014.

Broader Impacts

One of the major contributions of this research has been the establishment of methodologies to study the interaction of plasma with bio-molecules. In particular, our studies of atmospheric pressure plasma sources using very well-defined experimental conditions enabled to combine atomistic surface modifications of biomolecules with changes in their biological function. For example, development of methods to detect the effects of plasma treatment on immune-active biomolecules will be helpful in many future studies. Indeed, the results of this research benefits any field that requires well-controlled conditions, e.g. disinfection of packaging for food and medicines or decontamination of biological warfare agents, and has major implications for the emerging field of plasma medicine, where APP sources are found to induce wound healing and blood coagulation or therapeutically shrink cancerous tumors. Traditional cleaning and disinfection techniques used in hospitals suffer from several disadvantages that APP can potentially overcome due to its compatibility with heat-sensitive materials and use of relatively non-toxic gases. Our demonstration that mild, remote treatments that minimally etch the surfaces can cause various levels of oxidation, some of which appear to be generic to a wide variety of materials, is promising for sterilization or cleaning of very sensitive materials found in hospitals or ultra-clean environments. In addition,

this work guides the design of future APP sources since the plasma-environment interaction can be used to tune the density and type of reactive species striking a surface, which is required for specialized applications in plasma medicine.

This project contributed to the **graduate education** of four students, two of whom have graduated, and a third one who will graduate during the early part of 2015 with a PhD degree:

T.-Y. Chung (UCB) graduated in 2012 from UC Berkeley with a PhD

H.-W. Chang (UCB; visiting student from Taiwan – **not financially supported by this project**) graduated with a PhD from National Taiwan University

E. Bartis will graduate from University of Maryland in 2015 with a PhD

A. Knoll is a current PhD student at University of Maryland

Additionally, a number of undergraduate students were involved on a continuous basis in this project.

As a result, the project will have contributed excellent students to the workforce.

References:

[i] W. Van Gaens and A. Bogaerts, "Kinetic modelling for an atmospheric pressure argon plasma jet in humid air", Journal of Physics D-Applied Physics **46**, 275201 (2013)

[ii] E.A.J. Bartis, A.J. Knoll, P. Luan, C. Hart, D.B. Graves, J. Seog, and G.S. Oehrlein, "The Impact of Ambient Gas Chemistry on Polystyrene Surface Modification by Atmospheric Pressure Plasma", Plasma Processes and Polymers, (in prep, 2014).

[iii] J.F. Rabek, *Photodegradation of Polymers* (Springer, Berlin, 1996).

[iv] S. Gross and A. K. Bertram, "Reactive uptake of NO3, N2O5, NO2, HNO3, and O-3 on three types of polycyclic aromatic hydrocarbon surfaces," Journal of Physical Chemistry A **112**, 14 (2008).

[v] U. Kogelschatz, "Dielectric-barrier Discharges: Their History, Discharge Physics, and Industrial Applications", Plasma Chemistry and Plasma Processing **23**, 1 (2003).

[vi] S. Reuter, J. Winter, A. Schmidt-Bleker, D. Schroeder, H. Lange, N Knake, V. Schulz-von der Gathen, K.D. Weltmann, "Atomic oxygen in a cold argon plasma jet: TALIF spectroscopy in ambient air with modelling and measurements of ambient species diffusion", Plasma Sources Science and Technology **21**, 2 (2012).

[vii] A.J. Knoll, P. Luan, E.A.J. Bartis, C. Hart, Y. Raitses, and G.S. Oehrlein, "Real Time Characterization of Polymer Surface Modification by an Atmospheric Pressure Plasma Jet", Applied Physics Letters, (submitted, 2014).